



A review of 3D/2D registration methods for image-guided interventions

P. Markelj^{a,*}, D. Tomaževič^{a,b}, B. Likar^{a,b}, F. Pernuš^a

^a University of Ljubljana, Faculty of Electrical Engineering, Tržaška 25, 1000 Ljubljana, Slovenia

^b Sensum, Computer Vision Systems, Tehnološki park 21, 1000 Ljubljana, Slovenia

ARTICLE INFO

Article history:

Received 25 July 2009

Received in revised form 22 February 2010

Accepted 30 March 2010

Available online 13 April 2010

Keywords:

3D/2D registration

2D/3D registration

Review

Survey

Image-guided

ABSTRACT

Registration of pre- and intra-interventional data is one of the key technologies for image-guided radiation therapy, radiosurgery, minimally invasive surgery, endoscopy, and interventional radiology. In this paper, we survey those 3D/2D data registration methods that utilize 3D computer tomography or magnetic resonance images as the pre-interventional data and 2D X-ray projection images as the intra-interventional data. The 3D/2D registration methods are reviewed with respect to image modality, image dimensionality, registration basis, geometric transformation, user interaction, optimization procedure, subject, and object of registration.

© 2010 Elsevier B.V. All rights reserved.

1. Introduction

Image registration is one of the enabling technologies for image-guided radiation therapy (IGRT) (Jaffray et al., 2007, 2008), image-guided radiosurgery (IGRS) (Chang et al., 2003; Dieterich et al., 2008; Romanelli et al., 2006a) and image-guided minimally invasive therapy (IGMIT) which includes a wide variety of therapies in surgery (Peters, 2006; Germano, 2000; Peters and Cleary, 2008), endoscopy (Mayberg et al., 2005) and interventional radiology (Mauro et al., 2008). Registration is concerned with bringing the pre-intervention data (patient's images or models of anatomical structures obtained from these images and treatment plan) and intra-intervention data (patient's images, positions of tools, radiation fields, etc.) into the same coordinate frame (Peters, 2006; Sauer, 2005; Galloway, 2001; DiMaio et al., 2007; Yaniv and Cleary, 2006; Romanelli et al., 2006a,b; Avanzo and Romanelli, 2009). Currently, the pre-interventional data are three-dimensional (3D) computed tomography (CT) and magnetic resonance (MR) images, while the intra-intervention data are either two-dimensional (2D) ultrasound (US), projective X-ray (fluoroscopy), CT-fluoroscopy, and optical images, or 3D images like cone-beam CT (CBCT) and US, or 3D digitized points or surfaces. MR images are still seldom used intra-interventionally. With respect to intra-interventional data dimensionality, registration is thus either 3D/2D or 3D/3D.

All the above mentioned medical specialties benefit from image registration through easier and better guidance of an intervention

leading to reduced invasiveness and/or increased accuracy. In image-guided minimally invasive surgery, the registration of pre- and intra-interventional data and instrument tracking provide surgeon with information about the current position of his instruments relative to the planned trajectory, nearby vulnerable structures, and the ultimate target. In image-guided endoscopy, 3D virtual images of the anatomy and pathology are generated from pre-interventional images and registered to real-time live endoscopic images to provide augmented reality which enables display of anatomical structures that are hidden from the direct view by currently exposed tissues. In interventional radiology, registration of the pre-interventional image to the X-ray fluoroscopic or US image allows visualization of tools, like catheters and needles, in 3D which can greatly improve guidance. In external beam radiotherapy, registration of planning CT images and daily pre-treatment images allow precise patient positioning, which is of utmost importance for exact dose delivery to the target and for avoiding irradiation of healthy critical tissue. Throughout this survey the term image-guided interventions (IGI) is used to describe IGRT, IGRS, and IGMIT because, as already Peters and Cleary (2008) noted, IGI covers the widest range of surgical and therapeutic procedures. In the literature the terms image-guided therapy (IGT), image-guided surgery (IGS) and image-guided procedures (IGP) are often used instead of IGI.

The aim of this paper is to survey those 3D/2D data registration methods which use a 3D CT or MR pre-interventional image and one or more intra-interventional 2D X-ray projection images as sources of data to be registered. The 3D/3D registration methods where the intra-interventional image is a CBCT, CT, MR, or US

* Corresponding author.

E-mail address: primoz.markelj@fe.uni-lj.si (P. Markelj).

image (Jaffray et al., 2002; Pouliot et al., 2005; Jolesz, 2005; Penney et al., 2006) and 3D/2D volume-to-slice (Comeau et al., 2000; Wein et al., 2008; Micu et al., 2006; Birkfellner et al., 2007; Frühwald et al., 2009; Hummel et al., 2008; Fei et al., 2003) and (endoscopic) volume-to-video (Mori et al., 2002, 2005; Bricault et al., 1998; Deligianni et al., 2004, 2006; Burschka et al., 2005) registrations are beyond the scope of this review. Besides, registration methods that are based on intra-interventional data extracted from the patient’s skin surface or surfaces of exposed anatomical structures are also not reviewed. Nevertheless, other means of establishing 3D/2D registration that do not rely solely on X-ray images are mentioned where suitable. Although the term 2D/3D registration is more frequently used to describe registration in scope of this paper, we consistently use the term 3D/2D registration instead, since the 3D image is transformed to achieve the best possible correspondence with the 2D image(s), as shown in the following section.

2. Alignment of pre- and intra-interventional patient data

In IGI, registration is used to align the pre- and intra-interventional data just before and often also during an intervention in such a way that corresponding anatomical structures in the two data sets are aligned. The data sets to be registered are defined in distinct spaces or coordinate systems. The 3D pre-interventional data is defined in the data (image) coordinate system S_{pre} . The intra-interventional 3D data is defined either in some world (patient, treatment room) coordinate system S_w or data coordinate system S_{intra} , while the 2D intra-interventional data is always defined in data coordinate system S_{intra} (Fig. 1). If the intra-interventional data is defined in S_{intra} , a rigid transformation T_{calib} has to be defined by calibrating the intra-interventional data acquisition device to relate S_{intra} to S_w (Fig. 1) (van de Kraats et al., 2006; Livyatan et al., 2002; Hofstetter et al., 1999).

Let x_A^{3D} , x_B^{3D} , and x_{Bj}^{2D} , $j = 1, 2, \dots, N$, denote points of the pre-interventional data A , intra-interventional data B and N intra-interventional data B_j , defined over the domains $\Omega_A \subset \mathfrak{R}^3$, $\Omega_B \subset \mathfrak{R}^3$, and $\Omega_{Bj} \subset \mathfrak{R}^2$, $j = 1, 2, \dots, N$, respectively. Besides, let $A(x_A^{3D})$, $B(x_B^{3D})$, and $B_j(x_{Bj}^{2D})$, $j = 1, 2, \dots, N$, denote values of data A , B , and B_j , at positions x_A^{3D} , x_B^{3D} , and x_{Bj}^{2D} , $j = 1, 2, \dots, N$, respectively. The values can be intensities of the raw images or any data, even the points x_A^{3D} , x_B^{3D} , and x_{Bj}^{2D} , $j = 1, 2, \dots, N$, themselves, extracted from these images or obtained by other means (e.g., tracked

probe). Registration is concerned with finding the transformation T that defines the pose of S_{pre} in S_w (Fig. 1). The transformation T is found by transforming the data set $A(x_A^{3D})$ into $A^T(x_A^{3D})$ until $A^T(x_A^{3D})$ is best aligned with $B(x_B^{3D})$ or $B_j(x_{Bj}^{2D})$, $j = 1, 2, \dots, N$. A correct registration will allow any point defined in S_{pre} to be precisely located in S_w and/or S_{intra} . Depending on the type and dimensionality of data, the transformation T can be obtained by either 3D/3D image-to-patient, 3D/3D image-to-image, or 3D/2D image-to-image registration.

In case of 3D/3D image-to-patient registrations, no intra-interventional images are taken but corresponding isolated points or point clouds ($A(x_A^{3D}) = x_A^{3D}$, $B(x_B^{3D}) = x_B^{3D}$) representing surfaces, are determined in the pre-interventional image and patient, and registered (Peters, 2006):

$$T : A^T(x_A^{3D}) \iff B(x_B^{3D}). \quad (1)$$

Here, T is a spatial mapping because it maps only between coordinates. Isolated point-based registration methods use intrinsic anatomical landmarks (Zinreich et al., 1993; Colchester et al., 1996) or extrinsic markers integrated into a stereotactic frame (Galloway and Maciunas, 1990) or dental cast (Bale et al., 2000), skin-affixed (Colchester et al., 1996) or bone-implanted (Maurer et al., 1997). The landmarks and markers must be visible in pre-interventional images, while intra-interventionally their position is typically defined by a tracked probe. Registration methods that rely on surfaces match a digitized patient surface, obtained intra-interventionally by laser range scanning (Miga et al., 2003; Audette et al., 2003) or a stereo-based reconstruction method (Colchester et al., 1996; Sun et al., 2005), to the corresponding surface obtained by segmentation of the pre-interventional image.

In case of 3D/3D image-to-image registrations, patient images $B(x_B^{3D})$ like MR and CBCT images are acquired intra-interventionally (Jolesz, 2005; Jaffray et al., 2002; Pouliot et al., 2005). If the transformation T_{calib} is known, the relation of S_{intra} to S_w is also known, and the transformation T is defined by transforming the data set $A(x_A^{3D})$ into $A^T(x_A^{3D})$ until $A^T(x_A^{3D})$ is best aligned with $B(x_B^{3D})$:

$$T : A^T(x_A^{3D}) \iff B(x_B^{3D}). \quad (2)$$

In this case the transformation T is a more complete mapping than in the previous case because it incorporates image resampling and interpolation, and maps both positions and associated image values (Hill et al., 2001). The 3D/3D rigid and non-rigid mono- and multimodal registration problems are well studied and numerous good solutions are available (Maurer and Fitzpatrick, 1993; Maintz and Viergever, 1998; Hill et al., 2001; Pluim et al., 2003).

The term 3D/2D image-to-image registration can refer either to alignment of 3D spatial data to a single tomographic slice or to alignment of 3D spatial data to projective data (Maintz and Viergever, 1998).

In the first case, referred to as volume-to-slice registration, each value of the 2D slice image $B(x_B^{2D})$ from FluoroCT (Birkfellner et al., 2007; Frühwald et al., 2009; Micu et al., 2006), MRI (Fei et al., 2003) or US (Wein et al., 2008; Hummel et al., 2008; Comeau et al., 2000) obtained during the intervention, has a corresponding value in the 3D image $A(x_A^{3D})$ (one-to-one mapping) and as such can be considered an extreme case of 3D/3D registration where one of the images is reduced to a single slice. As in 3D/3D image-to-image registration, the relation between S_{intra} and S_w is defined by the transformation T_{calib} . The transformation T is defined by transforming the data set $A(x_A^{3D})$ into $A^T(x_A^{3D})$ until an oblique reformatted slice $A^T(x_A^{2D})$ taken from the high resolution 3D data set $A^T(x_A^{3D})$ is best aligned with image $B(x_B^{2D})$:

$$T : \mathcal{S}(A^T(x_A^{3D})) = A^T(x_A^{2D}) \iff B(x_B^{2D}), \quad (3)$$

where \mathcal{S} denotes the derivation of a reformatted slice from the 3D image data $A^T(x_A^{3D})$. In contrast, when aligning the 3D spatial data to

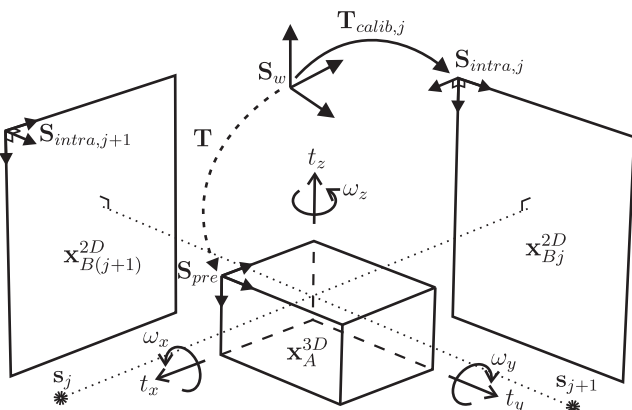


Fig. 1. Geometrical setup of the registration of a 3D image to two 2D X-ray projection images. s_j and s_{j+1} are the positions of the X-ray sources related to the j th and $(j+1)$ th 2-D images defined in coordinate systems $S_{intra,j}$ and $S_{intra,j+1}$, respectively. S_w is the world coordinate system and S_{pre} is the coordinate system of the pre-interventional 3D image. $T_{calib,j}$ are the rigid transformations between $S_{intra,j}$ and S_w . T is the transformation between S_{pre} and S_w that is searched for by registration. A rigid transformation T is defined by six parameters t_x , t_y , t_z , ω_x , ω_y and ω_z .

projective data, the one-to-one correspondence between 3D and 2D data is not valid and therefore fundamentally different registration approaches in comparison to volume-to-slice registration are required. In 3D/2D *image-to-image* registrations of 3D spatial and 2D projective data, N 2D patient images $B_j(\mathbf{x}_{B_j}^{2D})$, $j = 1, 2, \dots, N$, are acquired intra-interventionally. Again, if the transformation \mathbf{T}_{calib} is known, the relations of $\mathbf{S}_{intra,j}$ to \mathbf{S}_w are also known. Because of the different dimensions of the data sets to be registered, the transformation \mathbf{T} is defined by transforming the data set $A(\mathbf{x}_A^{3D})$ into $A^T(\mathbf{x}_A^{3D})$ until the projections of $A^T(\mathbf{x}_A^{3D})$ onto the domains Ω_{B_j} are best aligned with images $B_j(\mathbf{x}_{B_j}^{2D})$, $j = 1, 2, \dots, N$:

$$\mathbf{T} : \mathcal{P}_j(A^T(\mathbf{x}_A^{3D})) = A_j(\mathbf{x}_{A_j}^{2D}) \iff B_j(\mathbf{x}_{B_j}^{2D}), \quad \forall j, \quad (4)$$

or until $A^T(\mathbf{x}_A^{3D})$ is best aligned with the back-projections or reconstructions of $B_j(\mathbf{x}_{B_j}^{2D})$ into the domain Ω_A :

$$\mathbf{T} : A^T(\mathbf{x}_A^{3D}) \iff B_j(\mathbf{x}_{B_j}^{2D}) = \mathcal{B}_j(B_j(\mathbf{x}_{B_j}^{2D})), \quad \forall j, \quad (5)$$

or

$$\mathbf{T} : A^T(\mathbf{x}_A^{3D}) \iff B(\mathbf{x}_B^{3D}) = \mathcal{B}\{B_j(\mathbf{x}_{B_j}^{2D}), j = 1, 2, \dots, N\}, \quad (6)$$

respectively. The \mathcal{P}_j , $j = 1, 2, \dots, N$, are projection matrices defining projections of points in 3D onto each of the N 2D planes and are obtained by calibrating the intra-interventional imaging device (van de Kraats et al., 2006; Livyatan et al., 2002; Hofstetter et al., 1999). The \mathcal{B}_j , $j = 1, 2, \dots, N$, are corresponding back-projection matrices and \mathcal{B} is a reconstruction function. The transformation \mathbf{T} is again a complete mapping that incorporates image resampling and interpolation, and maps both positions and associated image values.

3. Survey of 3D/2D registration methods

Maintz and Viergever (1998) proposed a classification of image registration methods according to: image modality (Section 3.1), image dimensionality (Section 3.2), nature of the registration basis

(Section 3.3), geometric transformation (Section 3.4), user interaction (Section 3.5), optimization procedure (Section 3.6), subject (Section 3.7), and object of registration (Section 3.8). Publications, dealing with 3D/2D CT or MR to X-ray image registrations, are next reviewed in view of this classification.

3.1. Image modality

According to the image modalities involved, the reviewed 3D/2D registrations can be classified as *quasi-intra-modal*, *multi-modal* or *model-to-modality*. In *quasi-intra-modal* 3D/2D image registrations, CT is the pre-interventional modality and X-ray imaging is the intra-interventional modality. Although, the imaging principle in both modalities is the same, different photon energies and detector characteristics are used for image acquisition. Furthermore, other factors like scattered radiation and shading artifacts like the heel effect also contribute to differences in intensities. In *multi-modal* 3D/2D image registrations, MRI is used as the pre-interventional modality and X-ray imaging is the intra-interventional modality. For each of the modalities involved in quasi-intra-modal and multi-modal 3D/2D registrations, different acquisition protocols and contrast agents may be used. The X-ray images can be obtained at diagnostic energies (40–100 KeV) which yield high contrast X-ray images, or at treatment energies (2–20 MeV) yielding low contrast portal images. Depending on the X-ray energy, various types of X-ray detectors (image intensifier, digital X-ray detector, electronic portal imaging device) are available (Kirby and Glendinning, 2006). Since CT and X-ray imaging are based on the same principle and especially when they both acquire images at diagnostic energies, they are more closely related and thus easier to be registered than, for example, MR and X-ray images. The reviewed publications on 3D/2D CT to diagnostic X-ray image registration are given in Table 1, 1.a, publications on CT to portal image registration are given in Table 1, 1.b, while publications on MR to X-ray registrations are given in Table 1, 2.a. *Model-to-modality* 3D/2D registrations are used in cases when no

Table 1
Classification of 3D/2D registration methods according to image modality.

<i>1.a Quasi-intra-modal: CT to diagnostic X-ray</i>
Adler et al. (1999), Aouadi and Sarry (2008), Birkfellner et al. (2003, 2009), Byrne et al. (2004), Chen et al. (2007b, 2006, 2008), Cyr et al. (2000), Dennis et al. (2005), de Bruin et al. (2008), Dong et al. (2008), Feldmar et al. (1997), Florin et al. (2005), Fregly et al. (2005), Fu and Kuduvali (2008a, 2008b), Gong et al. (2006), Gottesfeld Brown and Boulton (1996), Groher et al. (2007b,a), Guezic et al. (1998, 2000), Hamadeh et al. (1998), Ho et al. (2007), Imamura et al. (2002), Jans et al. (2006), Jaramaz and Eckman (2006), Jin et al. (2006), Jonic et al. (2003), Kerrien et al. (1999), Kim et al. (2005, 2007), Knaan and Joskowicz (2003), Kubias et al. (2007), Lavallee and Szeliski (1995), Liao et al. (2006), Lemieux et al. (1994), Livyatan et al. (2003), Mahfouz et al. (2005), Markelj et al. (2008), Munbodh et al. (2006), Murphy (1997, 1999), Nakajima et al. (2002, 2007), Penney et al. (1998, 2001, 2007), Prümmer et al. (2006), Rohlfig et al. (2005a,b), Roth et al. (1999), Russakoff et al. (2003, 2005a), Russakoff et al. (2005b), Sundar et al. (2006), Tang et al. (2004b,a), Tomažević et al. (2003, 2007, 2006), Turgeon et al. (2005), Weese et al. (1997b, 1999), Wein et al. (2005), You et al. (2001), Zhang et al. (2006), Zheng et al. (2006b, 2008), Zöllei et al. (2001)
<i>1.b Quasi-intra-modal: CT to portal image</i>
Gilhuijs et al. (1996b), Clippe et al. (2003), Khamene et al. (2006), Bansal et al. (1999), Bansal et al. (2003), Chelikani et al. (2006), Aird and Conway (2002), Sirois et al. (1999), Sarrut and Clippe (2001), Remeijer et al. (2000), Munbodh et al. (2007), Munbodh et al. (2008, 2009), Kim et al. (2001)
<i>2.a Multi-modal: MR to diagnostic X-ray</i>
Alperin et al. (1994), Benameur et al. (2003, 2005a,b), Brunie et al. (1993), Bullitt et al. (1999), Chan et al. (2004), Chung et al. (2002), De Buck et al. (2005), Florin et al. (2005), Hipwell et al. (2003), Jomier et al. (2006), Kita et al. (1998), Liu et al. (1998), Markelj et al. (2007, 2008), McLaughlin et al. (2005), Miquel et al. (2006), Qi et al. (2008), Rhode et al. (2003, 2005), Rohlfig and Maurer (2002), Sundar et al. (2006), Tomažević et al. (2003, 2006), Zikic et al. (2008), Zheng et al. (2007), Vermandel et al. (2006), van de Kraats et al. (2005b)
<i>3.a Model-to-modality: 3D statistical model of anatomy to diagnostic X-ray</i>
Lamecker et al. (2006), Fleute and Lavallee (1999), Tang and Ellis (2005), Hurvitz and Joskowicz (2008), Sadowsky et al. (2006, 2007), Yao and Taylor (2003), Zheng et al. (2006a)
<i>3.b Model-to-modality: 3D geometrical model of an implant to diagnostic X-ray</i>
Banks and Hodge (1996), Fukuoka and Hoshino (1999), Hermans et al. (2007a), Hoff et al. (1998), Jaramaz and Eckman (2006), Kaptein et al. (2003), Wunsch and Hirzinger (1996), Yamazaki et al. (2004), Qi et al. (2008), LaRose (2001, 2000b), Mahfouz et al. (2003), Penney et al. (2007), Zuffi et al. (1999)

pre-interventional images are available, cannot be acquired, or are not needed. A model can be a 3D statistical model of an anatomy (Table 1, 3.a) or an exact 3D geometrical model of an implant (Table 1, 3.b).

3.2. Image dimensionality

To perform 3D/2D registration, the 3D and 2D data have to be brought into dimensional correspondence. Dimensional correspondence can be achieved either by transforming the 3D data into 2D or by transforming the 2D data into 3D. While the former approach leads to 2D/2D registration(s), the latter approach leads to a 3D/3D registration. More specifically, dimensional correspondence can be achieved either by the *projection*, *back-projection*, or *reconstruction* strategy.

By the *projection* strategy (Fig. 2), the 3D data is projected onto N planes Ω_{B_j} , $j = 1, 2, \dots, N$, of the intra-interventional 2D projection data $B_j(\mathbf{x}_{B_j}^{2D})$ using the N projection matrices \mathcal{P}_j , associated with $B_j(\mathbf{x}_{B_j}^{2D})$, $j = 1, 2, \dots, N$. The registration is then performed by optimizing the sum of criterion functions CF_j^{2D} , $j = 1, 2, \dots, N$:

$$\begin{aligned} \hat{\mathbf{T}} &= \arg \max_{\mathbf{T}} \sum_{j=1}^N CF_j^{2D} \\ &= \arg \max_{\mathbf{T}} \sum_{j=1}^N CF_j^{2D} (\mathcal{P}_j(A^{\mathbf{T}}(\mathbf{x}_A^{3D}), B_j(\mathbf{x}_{B_j}^{2D}))). \end{aligned} \quad (7)$$

By the *back-projection* strategy (Fig. 3), each of the N 2D intra-interventional data $B_j(\mathbf{x}_{B_j}^{2D})$ is back-projected into the 3D space using corresponding back-projection matrices \mathcal{B}_j , $j = 1, 2, \dots, N$. Similarly to the projection strategy, the registration is then performed by optimizing the sum of criterion functions CF_j^{3D} , $j = 1, 2, \dots, N$, each calculated on the basis of the 3D pre-interventional data and one of the back-projected intra-interventional 2D data:

$$\begin{aligned} \hat{\mathbf{T}} &= \arg \max_{\mathbf{T}} \sum_{j=1}^N CF_j^{3D} \\ &= \arg \max_{\mathbf{T}} \sum_{j=1}^N CF_j^{3D} (A^{\mathbf{T}}(\mathbf{x}_A^{3D}), \mathcal{B}_j(B_j(\mathbf{x}_{B_j}^{2D}))). \end{aligned} \quad (8)$$

By the *reconstruction* strategy (Fig. 4), a reconstruction function \mathcal{R} is used to reconstruct the 3D intra-interventional data $B(\mathbf{x}_B^{3D})$ from N

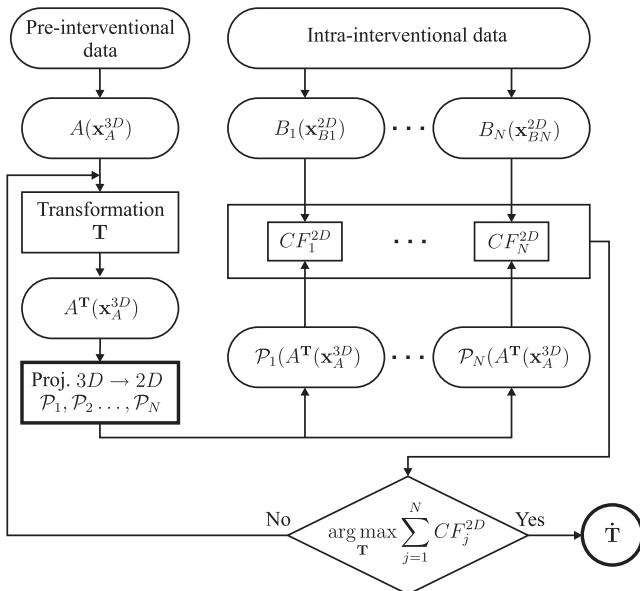


Fig. 2. 3D/2D registration based on projection strategy.

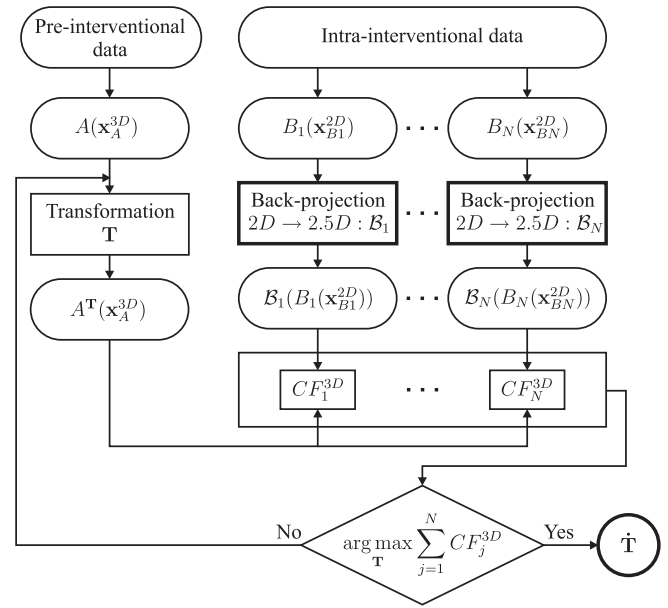


Fig. 3. 3D/2D registration based on back-projection strategy.

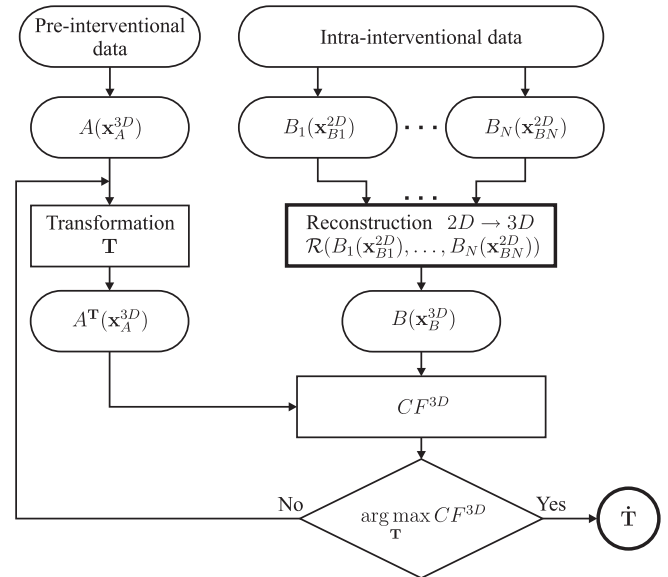


Fig. 4. 3D/2D registration based on reconstruction strategy.

2D intra-interventional data $B_j(\mathbf{x}_{B_j}^{2D})$: $B(\mathbf{x}_B^{3D}) = \mathcal{R}(B_1(\mathbf{x}_{B_1}^{2D}), \dots, B_N(\mathbf{x}_{B_N}^{2D}))$. Registration is then performed by optimizing the criterion function CF^{3D} calculated between the pre-interventional and the reconstructed 3D data:

$$\hat{\mathbf{T}} = \arg \max_{\mathbf{T}} CF^{3D} (A^{\mathbf{T}}(\mathbf{x}_A^{3D}), B(\mathbf{x}_B^{3D})). \quad (9)$$

In clinical practice, it is desired to keep the number of X-ray images to a minimum due to acquisition and reconstruction times and due to radiation exposure constraints. While in case of the projection and back-projection strategies one 2D image might be enough to achieve 3D/2D registration, the reconstruction approach requires at least two but preferably more 2D images to build a 3D image of sufficient quality to enable accurate and robust registration to the high-quality pre-interventional image. Generally, the more intra-interventional images are used for reconstruction the better is the registration accuracy. A detailed review of the 3D/2D

registration methods with respect to the described strategies and the nature of registration basis is given in the following Section 3.3.

3.3. Nature of registration basis

Regardless of the strategy for achieving dimensional correspondence, 3D/2D registration methods can be classified as *extrinsic*, *intrinsic* or *calibration-based*. The intrinsic methods are further classified as *feature-*, *intensity-* or *gradient-based*.

3.3.1. Extrinsic 3D/2D registration methods

Extrinsic methods rely on artificial objects like stereotactic frames (Jin et al., 2006) or a small number of markers attached to frames, dental casts, or implanted into bone (Gall et al., 1993; Tang et al., 2000), soft tissue (Shirato et al., 2000; Litzenberg et al., 2002; Aubry et al., 2004; Choi et al., 2005; Christie et al., 2005; Goodman and Koong, 2005; Mu et al., 2008; de Silva et al., 2006) or skin-affixed (Soete et al., 2002; Schweikard et al., 2004, 2005). Markers which are usually spheres (stainless steel beads, hollow plastic balls filled with an aqueous solution, gold seeds, etc.) are designed to be well detectable in images obtained by both the 3D and 2D imaging modalities. While stereotactic frames and bone implanted markers are rigidly attached to bone, skin markers and markers implanted into soft tissue can move due to skin elasticity or soft tissue deformation. In addition, markers may also migrate from their original implanted positions (Imura et al., 2005). Nevertheless, in radiation therapy and radiosurgery, marker-based registration is a common approach for patient positioning when irradiating tumors in soft tissues, such as those in the liver (Choi et al., 2005), lung (Schweikard et al., 2004, 2005; Christie et al., 2005; Shirato et al., 2000), prostate (Litzenberg et al., 2002; Aubry et al., 2004) and pancreas (Goodman and Koong, 2005), where there are no nearby bony structures to provide a reliable reference. All three strategies for achieving dimensional correspondence, have been used for marker-based 3D/2D registrations. In Shirato et al. (2000) the projection strategy was applied by which the positions of markers in a 3D image were projected into 2D where registration was performed. A back-projection strategy was applied by Tang et al. (2000). Virtual 3D rays were established by connecting each of the markers identified in 2D intra-interventional image with the X-ray source. Registration was then performed by rigidly transforming the markers found in the 3D pre-interventional image until their distance to the virtual rays was minimized. In Litzenberg et al. (2002) and Aubry et al. (2004) the reconstruction strategy was applied by which the 3D positions of markers were reconstructed from their positions in several 2D images and registered with markers found in the 3D pre-interventional image.

Registration of images based on extrinsic markers is straightforward, fast due to the sparse data, and does not require complex optimization algorithms. If point correspondences are known, several closed form solutions, which are optimal in the least squares sense, are most often used (Horn, 1987; Arun et al., 1987; Umeyama, 1991; Murphy, 2002; Skrinjar, 2006). Furthermore, error analysis and error prediction for these methods has been thoroughly studied (Fitzpatrick et al., 1998; Fitzpatrick and West, 2001). The most critical step of these methods is the identification or segmentation of markers, which is either performed manually or by using image processing techniques (Murphy et al., 2000; Mu et al., 2008). Although marker implantation requires an additional surgical procedure which is inconvenient and invasive to the patient, marker-based registrations are accurate and are therefore often used as a ground truth for validation of other registration methods (West et al., 1997). However, care must be taken since target registration error (TRE) (Fitzpatrick and West, 2001) is generally small near the markers, but can be quite large if markers are distant to the target. While the extrinsic methods can be very

effective, their main drawback is that they cannot be applied retrospectively as the markers must be attached before the pre-interventional images are acquired.

3.3.2. Intrinsic 3D/2D registration methods

Intrinsic registrations rely on images of anatomical structures. According to the intrinsic nature of registration, we propose a further classification into: *feature-*, *intensity-*, and *gradient-based* methods (Table 2). For each of these classes the projection, back-projection or reconstruction strategy can be used to achieve dimensional correspondence.

Feature-based 3D/2D registration methods are concerned with finding the transformation that minimizes the distances between 3D features, extracted from the pre-interventional image, or a model, and corresponding 2D features. The features are geometrical entities like isolated points or point sets, forming a curve, contour or surface. Extraction of geometrical features by image segmentation greatly reduces the amount of data, which in turn makes such registrations fast. However, the accuracy of a feature-based 3D/2D registration directly depends on the accuracy of segmentation, which by itself is a non-trivial procedure to perform automatically, while manual segmentation is time consuming and subjective. To reduce the influence of inaccurate segmentation, approaches for handling false geometrical correspondences and outliers were developed (Wunsch and Hirzinger, 1996; Guezic et al., 1998, 2000; Kita et al., 1998; Feldmar et al., 1997; Benameur et al., 2003, 2005a,b; Zheng et al., 2007; Groher et al., 2007a; Hamadeh et al., 1998). Feature-based methods can be further classified as point-to-point, curve-to-curve and surface-to-curve registrations.

The simplest feature-based 3D/2D registrations are point-to-point registrations of corresponding distinct anatomical landmarks located, usually by an operator, in both the 3D and 2D images. When point correspondences are established, extrinsic marker-based registration approaches can be applied (Bijhold, 1993). **Point-based 3D/2D registration methods are heavily dependent on the skills of the operator since it is difficult to find points in 2D that correspond to anatomical landmarks in 3D.** Nevertheless, this method often serves as a rough initial registration after which more sophisticated 3D/2D registration methods are applied (Roth et al., 1999; Benameur et al., 2003, 2005b; Hurvitz and Joskowicz, 2008; Zheng et al., 2006a; Zhang et al., 2006).

The problem of finding corresponding landmarks in 3D and 2D is avoided by curve-to-curve (Alperin et al., 1994; Bullitt et al., 1999; Feldmar et al., 1997; Florin et al., 2005; Groher et al., 2007b; Groher et al., 2007a; Kita et al., 1998; Zikic et al., 2008; Liu et al., 1998; Sundar et al., 2006) **and surface-to-curve¹ 3D/2D registrations using any of the dimensional correspondence strategies.** When the projection strategy is used (Table 2, 1.a; Fig. 5a), the distance between the projected 3D occluding contour or curve and the corresponding silhouette or curve in the 2D projection image is minimized.² **By the back-projection strategy (Table 2, 1.b; Fig. 5b), virtual rays are formed by connecting 2D points, representing an object's silhouette, a curve or edges, with the X-ray**

¹ Banks and Hodge (1996), Benameur et al. (2003), Benameur et al. (2005a), Benameur et al. (2005b), Feldmar et al. (1997), Fregly et al. (2005), Hoff et al. (1998), Kaptein et al. (2003), Lamecker et al. (2006), Murphy (1997), Murphy (1999), Brunie et al. (1993), Chen et al. (2006), Fleute and Lavalley (1999), Gilhuijs et al. (1996b), Guezic et al. (1998, 2000), Hamadeh et al. (1998), Lavalley and Szeliski (1995), Wunsch and Hirzinger (1996), Yamazaki et al. (2004), Zuffi et al. (1999), Cyr et al. (2000), Hermans et al. (2007a), Fukuoka and Hoshino (1999).

² Alperin et al. (1994), Banks and Hodge (1996), Benameur et al. (2003, 2005a,b), Bullitt et al. (1999), Feldmar et al. (1997), Florin et al. (2005), Fregly et al. (2005), Groher et al. (2007b,a), Hoff et al. (1998), Kaptein et al. (2003), Kita et al. (1998), Lamecker et al. (2006), Murphy (1997, 1999), Zikic et al. (2008), Liu et al. (1998), Cyr et al. (2000), Hermans et al. (2007a), Sundar et al. (2006), Fukuoka and Hoshino (1999), Zheng et al. (2007).

Table 2
Classification of intrinsic 3D/2D registration methods.

3D/2D registration classes	Pre-interventional 3D data	Intra-interventional 2D data	Dimensional correspondence strategy	References
<i>1. Feature-based</i>				
1.a	3D image → 3D feature (surface, model, points)	2D image → 2D feature (contours, points)	projection 3D → $N \times 2D$	^a
1.b	3D image → 3D feature (surface, model, points)	2D image → 2D feature (contours, points)	back-projection $N \times 2D \rightarrow 2.5D$	^b
1.c	3D image → 3D feature (model, points)	2D image → 2D feature (contours, points)	reconstruction $N \times 2D \rightarrow 3D$	^c
<i>2. Intensity-based</i>				
2.a	3D image	2D image	projection 3D → $N \times 2D$	^d
2.b	3D image → 3D segm. image	2D image	projection 3D → $N \times 2D$	^e
2.c	3D image	2D image → 3D image	reconstruction $N \times 2D \rightarrow 3D$	^f
<i>3. Gradient-based</i>				
3.a	3D image → 3D gradient	2D image → 2D gradient	projection 3D → $N \times 2D$	^g
3.b	3D image → 3D gradient	2D image → 2D gradient	back-projection $N \times 2D \rightarrow 2.5D$	^h
3.c	3D image → 3D gradient	2D image → 3D gradient	reconstruction $N \times 2D \rightarrow 3D$	ⁱ

^a Groher et al. (2007b), Florin et al. (2005), Feldmar et al. (1997), Fregly et al. (2005), Groher et al. (2007a), Cyr et al. (2000), Sundar et al. (2006), Alperin et al. (1994), Bullitt et al. (1999), Kita et al. (1998), Zikic et al. (2008), Liu et al. (1998), Zheng et al. (2007), Benameur et al. (2003, 2005a,b), Lamecker et al. (2006), Banks and Hodge (1996), Hoff et al. (1998), Kaptein et al. (2003), Hermans et al. (2007a), Fukuoka and Hoshino (1999).

^b Lavallee and Szeliski (1995), Chen et al. (2006), Feldmar et al. (1997), Guezic et al. (1998, 2000), Hamadeh et al. (1998), Gilhuijs et al. (1996b), Brunie et al. (1993), Fleute and Lavallee (1999), Wunsch and Hirzinger (1996), Yamazaki et al. (2004), Zuffi et al. (1999).

^c Zheng et al. (2006a).

^d Birkfellner et al. (2003, 2009), de Bruin et al. (2008), Byrne et al. (2004), Chen et al. (2007b), Fu and Kuduvali (2008b,a), Gong et al. (2006), Lemieux et al. (1994), Ho et al. (2007), Imamura et al. (2002), Jaramaz and Eckman (2006), Jonic et al. (2003), Kerrien et al. (1999), Kim et al. (2005, 2007), Knaan and Joskowicz (2003), Liao et al. (2006), Munbodh et al. (2006), Murphy (1997, 1999), Nakajima et al. (2002, 2007), Penney et al. (1998, 2001, 2007), Rohlfing et al. (2005a,b), Roth et al. (1999), Russakoff et al. (2003, 2005a,b), Tang et al. (2004b), Tang et al. (2004a), Weese et al. (1997b, 1999), Zhang et al. (2006), Zheng et al. (2006b, 2008), Zöllei et al. (2001), You et al. (2001), Dong et al. (2008), Kubias et al. (2007), Clippe et al. (2003), Khamene et al. (2006), Kim et al. (2001), Munbodh et al. (2007, 2008, 2009), Sarrut and Clippe (2001), Gottesfeld Brown and Boulton (1996), Jans et al. (2006), Sirois et al. (1999), Hipwell et al. (2003), McLaughlin et al. (2005), Qi et al. (2008), Rohlfing and Maurer (2002), LaRose (2001), LaRose et al. (2000b), Dey and Napel (2006).

^e Aouadi and Sarry (2008), Chen et al. (2008), Dennis et al. (2005), Turgeon et al. (2005), Bansal et al. (1999, 2003), Chelikani et al. (2006), Chan et al. (2004), Vermandel et al. (2006), Jomier et al. (2006), Tang and Ellis (2005), Yao and Taylor (2003), Hurvitz and Joskowicz (2008), Sadowsky et al. (2006, 2007), Mahfouz et al. (2003).

^f Tomažević et al. (2006), Prümmer et al. (2006).

^g Livyatan et al. (2003), Wein et al. (2005).

^h Tomažević et al. (2003), van de Kraats et al. (2005b), Tomažević et al. (2007).

ⁱ Markelj et al. (2008).

source. Registration is performed in 3D by minimizing either the distance between the 3D geometrical structure and virtual rays (Feldmar et al., 1997; Brunie et al., 1993; Chen et al., 2006; Fleute and Lavallee, 1999; Guezic et al., 1998, 2000; Hamadeh et al., 1998; Lavallee and Szeliski, 1995; Wunsch and Hirzinger, 1996; Yamazaki et al., 2004; Zuffi et al., 1999) or distances that the virtual rays pass through the pre-segmented 3D (bony) structures (Gilhuijs et al., 1996b). Zheng et al. (2006a) proposed an approach that in an iterative fashion combines the projection and reconstruction strategies (Table 2, 1.b; Fig. 5c). First, contours of a surface defined by a point distribution model are projected onto several 2D image planes where corresponding edge points are found. These are then back-projected into 3D, reconstructed into a 3D point set, and registered to the corresponding 3D point set by non-rigidly deforming the point distribution model.

Point correspondences must be established to be able to determine the distances between geometrical features. Point correspondences are most commonly obtained by finding minimal Euclidian distances between points with approaches like or similar to the one applied in the iterative closest point (ICP) (Besl and McKay, 1992) approach.³ Thereby, the registration problem is cast

as an iterative procedure alternating the correspondence and transformation steps. In the correspondence step, the point correspondences are determined, while in the transformation step the position of the 3D data is updated with the incremental transformation obtained by closed form registration of the corresponding point pairs obtained in the first step. Alternatively, distance maps can be built and implicit correspondences determined from the distances pre-calculated and stored in a distance map (Benameur et al., 2003, 2005a,b; Florin et al., 2005; Lavallee and Szeliski, 1995; Zuffi et al., 1999; Yamazaki et al., 2004; Sundar et al., 2006; Fukuoka and Hoshino, 1999). Since both of these approaches are sensitive to outlier points, robust methods like the M-estimator (Wunsch and Hirzinger, 1996), Tukey weighting function (Guezic et al., 1998, 2000), the Voronoi diagram (Kita et al., 1998) or Extended Kalman Filter (Feldmar et al., 1997) have been implemented to reduce the effect of outlier data. Furthermore, outliers can also be rejected by using the directional correspondence between the curves (Feldmar et al., 1997), i.e. the angle between the tangents on the curves at corresponding points, or the directional information between the curves and the surface (Guezic et al., 2000; Benameur et al., 2003, 2005a,b; Zheng et al., 2007), i.e. the angle between the normal to the curve and normal to the surface at corresponding points. The ICP-like approach can also be extended into a statistical framework, where instead of treating the correspondence as a binary variable, a probabilistic approach to assigning correspondences is used and a cooperative approach between

³ Alperin et al. (1994), Brunie et al. (1993), Fregly et al. (2005), Bullitt et al. (1999), Chen et al. (2006), Feldmar et al. (1997), Fleute and Lavallee (1999), Groher et al. (2007b), Guezic et al. (1998, 2000), Kaptein et al. (2003), Kita et al. (1998), Lamecker et al. (2006), Liu et al. (1998), Wunsch and Hirzinger (1996), Zheng et al. (2007).

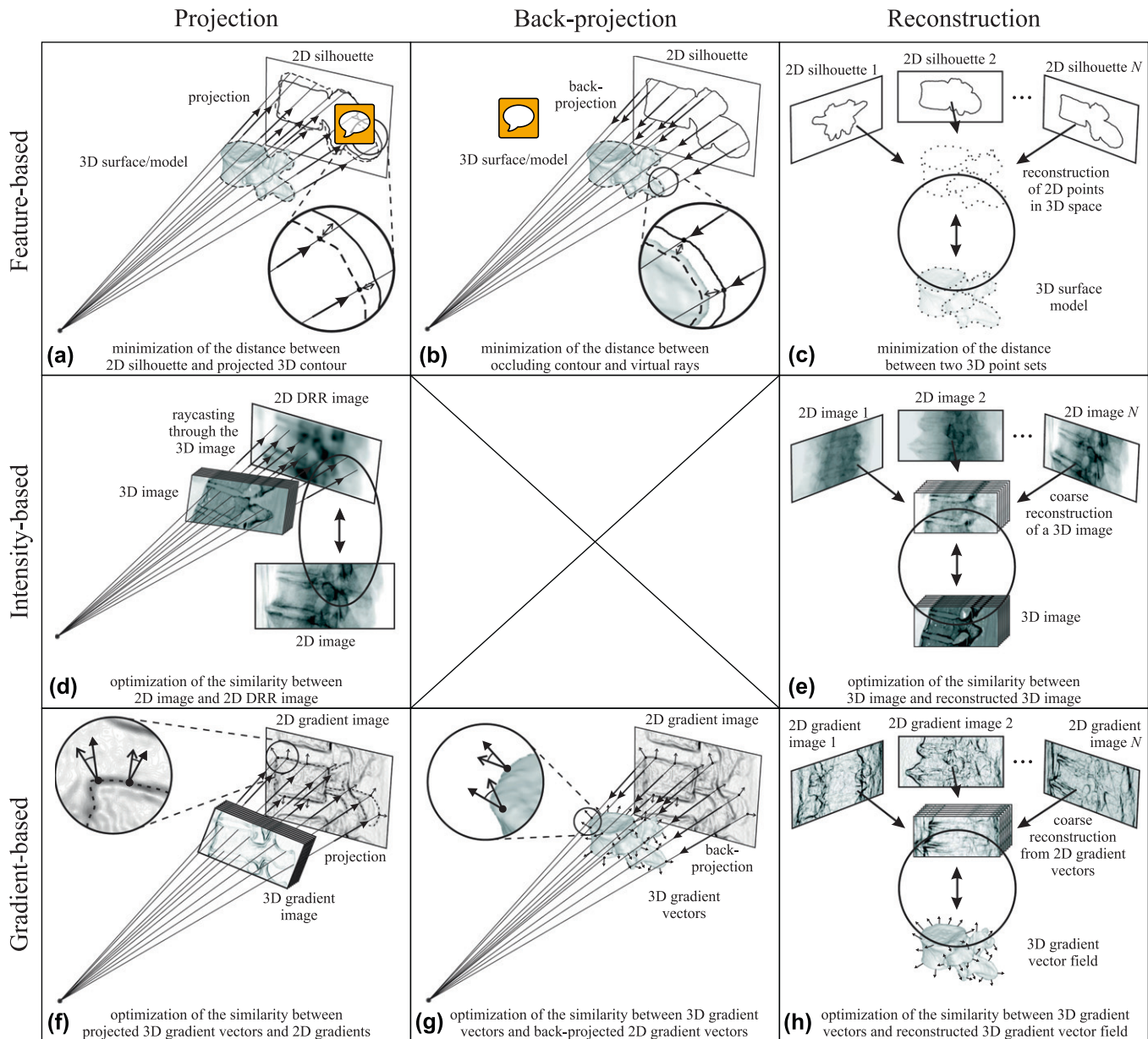


Fig. 5. Geometrical setup of 3D/2D registration methods according to the nature of the registration basis and strategy to achieve spatial correspondence.

segmentation and registration is applied (Groher et al., 2007a; Hamadeh et al., 1998).

Correspondences between features can also be established in 2D by using library-based registrations (Section 3.6). First, a library of 2D templates is generated for a predefined set of transformation parameters, which are generally the out-of-plane translation and rotations. Each library template thus represents the 3D geometric feature's expected 2D appearance for a particular transformation. The template that is most similar to the 2D geometric feature defines the out-of-plane transformation parameters. The chosen template is then aligned with the 2D data to define the remaining unknown transformation parameters. Templates, used in 3D/2D registration, can be Fourier descriptors of a 2D silhouette (Banks and Hodge, 1996), shock graph representation of the projected 3D shape (Cyr et al., 2000), 2D silhouettes (Hermans et al., 2007a), or 2D binary projection images (Hoff et al., 1998). The most similar of these templates in the library is determined by searching for optimal Fourier coefficients (Banks and Hodge, 1996), by graph matching (Cyr et al., 2000), by template matching of the bending

patterns of the contour (Hermans et al., 2007a), or by the minimal shape difference between the template and the 2D binary image, respectively. Although, the accuracy of the final alignment can be increased by registration of the template and the 2D data or interpolation between the closest template samples (Banks and Hodge, 1996), registration accuracy of library-based procedures is limited to the resolution of the template. Therefore, to make these methods computationally feasible, limitations regarding the pose of the object must be imposed which makes them more suitable for registration initialization (Hermans et al., 2007a,b).

Intensity-based 3D/2D registrations rely solely on information contained in voxels and pixels of 3D and 2D images, respectively. In contrast to feature-based methods, the coinciding points are considered to be the corresponding points and instead of the distance, the similarity measure, calculated using pixel-wise comparison, defines the correspondence between 3D pre- and 2D intra-interventional images. Intensity-based methods are further classified according to the strategy for achieving dimensional correspondence (Section 3.2) and strategies to reduce the amount of data.

By far the most reported 3D/2D registration method in literature is based on simulated X-ray projection images called digitally reconstructed radiographs (DRRs). These are produced from a CT image using ray-casting (Table 2, 2.a; Fig. 5d) (Goitein et al., 1983). Similarly as DRR, a maximum intensity projection (MIP) can also be generated from a CT image by projecting the maximum intensity value onto the 2D plane (Kerrien et al., 1999). The registration of a CT volume relative to an X-ray image is estimated by iteratively optimizing the similarity measure calculated between a DRR (MIP) generated for the current transformation and an X-ray image.⁴ The most frequently used and studied similarity measures for DRR-based 3D/2D registrations are mutual information,⁵ (normalized) cross correlation,⁶ sum of square differences (Fu and Kuduvali, 2008b; Jonic et al., 2003; Zheng et al., 2006b, 2008; Jans et al., 2006; Khamene et al., 2006), entropy of difference image (Kim et al., 2007; Penney et al., 1998; Russakoff et al., 2003; Hipwell et al., 2003), as measures of global intensity correspondence, and pattern intensity,⁷ gradient correlation (de Bruin et al., 2008; Kim et al., 2007; Lemieux et al., 1994; Nakajima et al., 2002; Penney et al., 1998; Russakoff et al., 2003; Tang et al., 2004b,a; Gottesfeld Brown and Boulton, 1996; Khamene et al., 2006; Hipwell et al., 2003), and gradient difference (Byrne et al., 2004; Imamura et al., 2002; Kim et al., 2007; Nakajima et al., 2007; Penney et al., 1998, 2001, 2007; Russakoff et al., 2003; Khamene et al., 2006; Hipwell et al., 2003; McLaughlin et al., 2005), as measures of correspondence of local intensity changes. Other measures, such as variance weighted sum of local normalized correlation (LaRose, 2001, 2000b; Knaan and Joskowicz, 2003; Khamene et al., 2006), normalized mutual information (Jans et al., 2006; Chen et al., 2007b), chi-square (Clippe et al., 2003; Sarrut and Clippe, 2001; Murphy, 1997, 1999) and correlation ratio (Clippe et al., 2003; Khamene et al., 2006), were also applied, while Dong et al. (2008) showed the feasibility of constructing a similarity measure using coefficients from an orthogonal set of base functions by decomposing X-ray and DRR images under comparison into orthogonal Zernike moments. Furthermore, a unifying framework for developing new similarity measures based on Markov random field modeling of difference images was proposed (Zheng et al., 2006b). From studies comparing different similarity measures (Kim et al., 2007; Khamene et al., 2006; Penney et al., 1998; Clippe et al., 2003; Hipwell et al., 2003; Russakoff et al., 2003; Imamura et al., 2002; Birkfellner et al., 2009; Munbodh et al., 2009), it can be concluded that similarity

measures based on global intensity correspondence are less suitable for matching DRRs with X-ray images. The measures of correspondence of local intensity changes produce more accurate and reliable results, although in some studies mutual information proved to be among the best measures, especially when registering real images (Aouadi and Sarry, 2008; Russakoff et al., 2003; Kim et al., 2007). Therefore, despite the large body of research devoted to finding the optimal similarity measure for 3D/2D registration it seems that the best similarity measures for 3D/2D registration will have to be specifically adapted to the nature of the relationship between the intensities of the DRR and the X-ray images and/or to the understanding of the image formation process. Such similarity measures were most recently proposed by Birkfellner et al. (2009) and Munbodh et al. (2009). Birkfellner et al. (2009) recognized the quasi-intra-modal nature of 3D/2D registration and proposed a similarity measure called stochastic rank correlation that is based on the Spearman's rank correlation coefficient and on statistical modeling of the intensity values. The measure is invariant to differences in image intensities that arise between DRRs and X-ray images, while the stochastic random sampling enables the registration with as little as 5% of image data. In contrast, Munbodh et al. (2009) formulated similarity measures which are tailored to the statistics of the CT and X-ray image acquisition. Thereby, Poisson and Gaussian probability distributions were used to model the distribution of intensity values of the two modalities derived from the Poisson nature of photon noise present during the acquisition of transmission images. New similarity measures were calculated from the assumed distributions using the maximum likelihood estimation.

One drawback of DRR-based 3D/2D registration is that it is generally not suitable for registration of MR and X-ray images because there is practically no correspondence between MR generated DRRs and X-ray images, except in cases when contrast agents are applied (Hipwell et al., 2003; McLaughlin et al., 2005), or DRRs of segmented MR images (Yin et al., 1998; Chen et al., 2007a) are used. Another drawback of DRR-based methods is that by projecting a high-quality 3D CT image into 2D, valuable 3D information may be lost. To overcome this deficiency, Rohlfing and Maurer (2002) proposed a probabilistic extension to the computation of DRRs that preserves much of the spatial separability of tissues along the virtual rays. To match the probabilistic DRR to the X-ray image they applied an entropy similarity measure computed from probabilistic images. The advantage of DRR-based methods is that they require little or no segmentation and therefore do not suffer from segmentation errors. Moreover, since these methods utilize all the information in the images, it is reasonable to expect that they are more accurate than feature-based methods. In the comparative study of McLaughlin et al. (2005) on feature- and DRR-based 3D/2D registrations of phase-contrast MRA (PC-MRA) and 2D digital subtraction angiographs (DSA), the authors showed that the DRR-based method was more accurate and reliable than the feature-based method. Nevertheless, it has to be noted, that due to numerous local maxima of intensity or gradient-based similarity measures, DRR-based methods have a small capturing range and therefore require initialization close to the searched pose (Liviyatan et al., 2003; van de Kraats et al., 2005a; Aouadi and Sarry, 2008; Fu and Kuduvali, 2008b), which can be achieved by other, less accurate, means of patient positioning (Fu and Kuduvali, 2008b; Khamene et al., 2006; Clippe et al., 2003; Dey and Napel, 2006; Ho et al., 2007; Jans et al., 2006).

A further clinical constraint of registrations employing DRRs, is the computational complexity of DRR generation when using standard ray-casting in every iteration of the optimization. The high computational cost of volume rendering has long been a focus of research in the computer graphics and computer vision communities (Cabral et al., 1994; Levoy and Hanrahan, 1994; Rezk-Salama et al., 2000). Over the years the advances in the two fields were

⁴ Clippe et al. (2003), Chen et al. (2007b), de Bruin et al. (2008), Byrne et al. (2004), Dey and Napel (2006), Fu and Kuduvali (2008b,a), Birkfellner et al. (2003, 2009), Penney et al. (1998), Lemieux et al. (1994), Gong et al. (2006), Gottesfeld Brown and Boulton (1996), Hipwell et al. (2003), Ho et al. (2007), Imamura et al. (2002), Jans et al. (2006), Jaramaz and Eckman (2006), Jonic et al. (2003), Khamene et al. (2006), Kim et al. (2001), Kim et al. (2005, 2007), Knaan and Joskowicz (2003), LaRose (2001, 2000b), Liao et al. (2006), McLaughlin et al. (2005), Munbodh et al. (2006, 2007, 2008, 2009), Nakajima et al. (2002, 2007), Penney et al. (2001, 2007), Rohlfing et al. (2005a,b), Roth et al. (1999), Russakoff et al. (2003, 2005a,b), Sarrut and Clippe (2001), Sirois et al. (1999), Tang et al. (2004b,a), Weese et al. (1997b, 1999), You et al. (2001), Zhang et al. (2006), Zheng et al. (2006b, 2008), Zöllei et al. (2001), Dong et al. (2008), Kubias et al. (2007), Kerrien et al. (1999), Qi et al. (2008), Murphy (1997, 1999).

⁵ Kim et al. (2005, 2007), Liao et al. (2006), Penney et al. (1998), Rohlfing et al. (2005b), Russakoff et al. (2003, 2005a,b), Zheng et al. (2006b), Zheng (2008), Zöllei et al. (2001), Dey and Napel (2006), Clippe et al. (2003), Khamene et al. (2006), Kim et al. (2001), Munbodh et al. (2007), Sarrut and Clippe (2001), Hipwell et al. (2003).

⁶ Birkfellner et al. (2009), de Bruin et al. (2008), Kerrien et al. (1999), Gong et al. (2006), Kim et al. (2007), Knaan and Joskowicz (2003), Lemieux et al. (1994), Munbodh et al. (2006), Penney et al. (1998), Russakoff et al. (2003), You et al. (2001), Jans et al. (2006), Clippe et al. (2003), Khamene et al. (2006), Kim et al. (2001), Munbodh et al. (2007, 2009), Sarrut and Clippe (2001), Hipwell et al. (2003), LaRose et al. (2000a).

⁷ Birkfellner et al. (2003), Birkfellner et al. (2009), Fu and Kuduvali (2008b), Fu and Kuduvali (2008a), Ho et al. (2007), Kim et al. (2007), Liao et al. (2006), Penney et al. (1998, 2001), Rohlfing et al. (2005a), Russakoff et al. (2003), Weese et al. (1997b, 1999), Dey and Napel (2006), Khamene et al. (2006), Sirois et al. (1999), Hipwell et al. (2003).

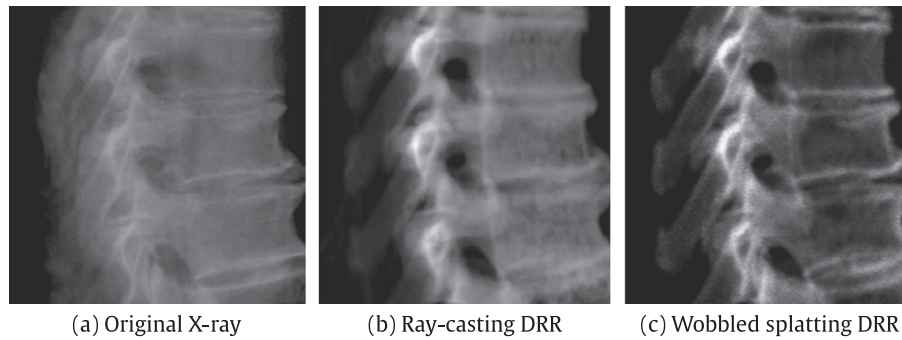


Fig. 6. Comparison of the original X-ray image (a) to DRR images generated at the ground truth position of the CT image with ray-casting (b) and wobbled splatting (c).

adopted for medical image registration and also several other approaches for faster DRR generation were proposed. They can be roughly divided into software- and hardware-based approaches. The software-based approaches propose more efficient rendering algorithms such as shear-warp factorization (Weese et al., 1999; Göcke et al., 1999), the transgraph (LaRose, 2001; Knaan and Joskowicz, 2003), adaptive Monte Carlo volume rendering (Li et al., 2006), attenuation fields (Russakoff et al., 2005b), progressive attenuation fields (Rohlfing et al., 2005b) or wobbled splatting (Birkfellner et al., 2005b, 2009). While the first four approaches require pre-computation, the latter two do not. Two- to thirty-fold improvement of speed was reported by Russakoff et al. (2005b). An illustration of the quality of the DRR images generated with ray-casting and wobbled splatting (Birkfellner et al., 2005b) in reference to the X-ray image using the publicly available spine phantom image data (van de Kraats et al., 2005a) is given in Fig. 6. To further reduce the computation time, hardware-based approaches can be used, employing fast rendering using the computer's graphic card (LaRose, 2001; Gong et al., 2006; Jaramaz and Eckman, 2006; Khamene et al., 2006; Kim et al., 2005; Liao et al., 2006; Tang et al., 2004b,a; You et al., 2001; Kubias et al., 2007; Spoerk et al., 2007) and/or massive parallelization (Spoerk et al., 2007; Wein et al., 2005). These approaches alone can improve the speed of registration up to 25 times (Tang et al., 2004a). Other approaches to faster generation of DRRs involved pre-computation of a subspace of DRRs according to the expected range of transformation parameters (Clippe et al., 2003; Fu and Kuduvalli, 2008b; Jans et al., 2006; Roth et al., 1999; Sarrut and Clippe, 2001), decoupling transformation parameters using an appropriate world coordinate system (Birkfellner et al., 2003; Fu and Kuduvalli, 2008b; Fu and Kuduvalli, 2008a; Jans et al., 2006; Kubias et al., 2007), efficient implementation of histogram-based stochastic techniques (Zöllei et al., 2001), and the use of sophisticated minimization strategies to minimize the number of iterations (Zöllei et al., 2001; Knaan and Joskowicz, 2003; Dey and Napel, 2006; Gong et al., 2006; Fu and Kuduvalli, 2008b; Aouadi and Sarry, 2008; Lemieux et al., 1994). Finally, the computational problem may also be reduced by calculating DRRs containing only structures of interest.⁸

In order to avoid the computational disadvantages of DRR-based intensity methods, a new group of intensity-based methods emerged recently that reduce the amount of data by segmenting the 3D image before the projection strategy is applied (Table 2,

2.b). Segmentation of the 3D image(s) is performed to extract either a (surface) model (Aouadi and Sarry, 2008; Chan et al., 2004, 2008; Dennis et al., 2005; Jomier et al., 2006; Mahfouz et al., 2003; Turgeon et al., 2005; Vermandel et al., 2006) or build a statistical model (Tang and Ellis, 2005; Yao and Taylor, 2003; Hurvitz and Joskowicz, 2008; Sadowsky et al., 2006, 2007), while the registration framework remains the same as in the classic DRR-based registration. This group of methods was referred to as *hybrid* (Turgeon et al., 2005; Vermandel et al., 2006) because of the combination of segmentation, typical of feature-based methods, and pixel-wise comparison, typical of intensity-based methods. Different methods have been proposed for construction of DRRs of segmented data. DRRs were formed by ray-casting either through a tetrahedral mesh model rendered with density functions (Yao and Taylor, 2003; Sadowsky et al., 2006, 2007; Hurvitz and Joskowicz, 2008), through a surface model using a CT attenuation map (Aouadi and Sarry, 2008), or by using the z-buffer, which was based on the distance that a projection ray traversed through a 3D surface model (Vermandel et al., 2006). A binary DRR image was calculated as a MIP in Turgeon et al. (2005) and Chan et al. (2004), while in Chen et al. (2008) strips of intensities orthogonal to the projected contour were formed by ray-casting. To register DRRs and X-ray, images several similarity measures like gradient correlation (Aouadi and Sarry, 2008; Yao and Taylor, 2003; Tang and Ellis, 2005), (normalized) mutual information (Sadowsky et al., 2006, 2007), and gradient difference (Hurvitz and Joskowicz, 2008) were used, while intensity and contour matching scores in the local neighborhood of the projected contour were proposed in Dennis et al. (2005) and Mahfouz et al. (2003). Furthermore, in Jomier et al. (2006) vessels were registered by optimizing the sum of the Gaussian-blurred intensity values at positions defined by virtual rays traversing a 3D (vessel) model, while weighting of the projected intensity values was provided by the 3D distance of the virtual ray through the model.

More advanced approaches combined registration and segmentation procedures into an iterative framework (Bansal et al., 1999, 2003; Chelikani et al., 2006). In these procedures, the current estimated registration was used to drive the segmentation, which in turn enabled the computation of a new registration estimate. The aim of the segmentation was not to extract features, but rather to extract information that is vital for registration and at the same time perform data reduction (Bansal et al., 1999, 2003; Chelikani et al., 2006; Aouadi and Sarry, 2008; Chan et al., 2004, 2008; Dennis et al., 2005; Jomier et al., 2006; Mahfouz et al., 2003; Turgeon et al., 2005), or segmentation was used to generate a statistical model of the anatomy of interest and thereby avoid the need for 3D image acquisition (Tang and Ellis, 2005; Yao and Taylor, 2003; Hurvitz and Joskowicz, 2008; Sadowsky et al., 2006, 2007).

⁸ Byrne et al. (2004), de Bruin et al. (2008), Dey and Napel (2006), Fu and Kuduvalli (2008b,a), Hipwell et al. (2003), Ho et al. (2007), Imamura et al. (2002), Jans et al. (2006), Khamene et al. (2006), Knaan and Joskowicz (2003), Munbodh et al. (2006, 2008, 2009), Nakajima et al. (2002), Penney et al. (1998, 2001, 2007), Roth et al. (1999), Russakoff et al. (2003), Russakoff et al. (2005a,b), Sirois et al. (1999), Rohlfing et al. (2005a,b, 2002), Tang et al. (2004b,a), Weese et al. (1997b, 1999), Zhang et al. (2006).

Few intensity-based methods utilize the reconstruction strategy (Tomažević et al., 2006; Prümmer et al., 2006) (Table 2, 2.c; Fig. 5e). This approach is similar to the CBCT approach, except that a 3D image is reconstructed from only a few 2D X-ray images. A high-quality kV (Jaffray et al., 2002) or MV (Pouliot et al., 2005) CBCT requires more than 100 projection images and can be easily registered to a pre-interventional 3D image using e.g. mutual information as the similarity measure (Pouliot et al., 2005). An interesting question however is, what is the minimal number of X-ray images from which a 3D image can be reconstructed that still contains enough information for accurate registration with the high-quality pre-interventional image. Tomažević et al. (2006) demonstrated on his method that a CT of a spine segment can be registered to a 3D image reconstructed from as few as two X-ray images. To overcome the problem of poor quality of a 3-D image reconstructed from only a few fluoroscopic X-ray images, a robust mutual information based similarity measure, called asymmetric multi-feature mutual information, that used additional spatial features in the form of intensity gradients was proposed (Tomažević et al., 2006). This method allows registration of MR to X-ray images as well. However, due to larger differences between the MR and X-ray images, the 3D image had to be reconstructed from more X-ray images then in the case of CT to X-ray registration.

Gradient-based methods were simultaneously introduced by Tomažević et al. (2003) and Livyatan et al. (2003). Both approaches are based on the fact that rays emanating from the X-ray source that point to edges in the X-ray images are tangent to surfaces of distinct anatomical structures. Therefore, when the CT (MR) image is aligned with the corresponding anatomy, the rays pass through local magnitude maxima of the 3D CT (MR) gradient vector field. By using a simplified model of X-ray generation, Tomažević et al. (2003) and Livyatan et al. (2003) derived the gradient projection relationship that exists between gradients of attenuation coefficients and X-ray image intensity gradients. According to the gradient projection relationship, the gradient of the point in the X-ray image is equal to the integral over the weighted projections of volume gradients onto the image plane. The weight is the relative distance of the 3D point from the X-ray source. Knowing how the attenuation coefficient gradient is projected to a point on the detector (imaging) plane, the image intensity gradient at this point can be back-projected toward the X-ray source to obtain a back-projected gradient at any location along the beam (Table 2, 3.b; Fig. 5g). The method of Tomažević et al. (2003) requires that a 3D gradient vector field (surface normals) is first extracted from CT or MR image. During each step of the iterative 3D/2D registration procedure, 2D gradient vectors of X-ray images are extracted at locations defined by rays emanating from the X-ray source and passing through the current position of 3D points which have

high gradient magnitudes, and back-projected to these 3D points. The rigid 3D/2D registration transformation is defined by the best match between 3D gradient vectors and back-projected gradients, concerning their magnitudes and especially directions. To increase the accuracy and reliability of MR to X-ray registrations, a mapping function was proposed by van de Kraats et al. (2005b) to generate CT-like data from the MR data. The method of Livyatan et al. (2003) also requires that a 3D gradient field is first extracted from a CT image. In contrast to the back-projection approach of Tomažević et al. (2003), Livyatan et al. (2003) found the optimal rigid transformation by rigidly transforming the 3D gradient vector field until the sum of magnitudes of projected 3D gradients, which were incident to the rays that emanated from the X-ray source and pointed to edge pixels extracted from the 2D image, were maximized (Table 2, 3.a; Fig. 5f). The influence of 2D outlier edges was eliminated by setting the magnitude of the gradient projection to zero when its direction diverged in comparison to the 2D gradient direction.

A gradient projection-based method similar to the DRR method was introduced by Wein et al. (2005). A 3D gradient image was calculated and 3D gradients above a user set threshold were projected into 2D and matched with the 2D gradient image using the gradient correlation similarity measure (Penney et al., 1998). The authors proposed to use gradient ray-casting or gradient splatting for projecting the gradients. Since only gradients above a threshold were projected, registration could be performed about 10 times faster than with the intensity ray-casting approach. Most recently, Markelj et al. (2008) presented a gradient-based method where the reconstruction strategy was used to achieve dimensional correspondence (Table 2, 3.c; Fig. 5h). Thereby, 3D and 2D gradient vector fields were first extracted from a 3D CT or MR image and 2D X-ray images, respectively. A coarsely reconstructed 3D gradient field was formed by simply adding the back-projected 2D gradient vectors from all available 2D images (see Fig. 7). In this way, the 3D/2D registration problem was transformed into the problem of registering two 3D gradient vector fields. The correspondences between the two gradient vector fields were established by searching in the directions of gradients of the 3D image using the similarity measure proposed in Tomažević et al. (2003). To avoid the problem of false gradient vector correspondences, the authors employed the random sample consensus algorithm (RANSAC) to pick a good set of correspondences before continuing with the registration. Finally, the search space was reduced from a coarse to a fine scale, where the final registration was achieved by optimizing the gradient-based similarity measure (Tomažević et al., 2003).

3.3.3. Calibration-based 3D/2D registration methods

A 3D/2D registration can also be *calibration-based*. The recent emergence of hybrid 2D X-ray and 3D MR imaging systems

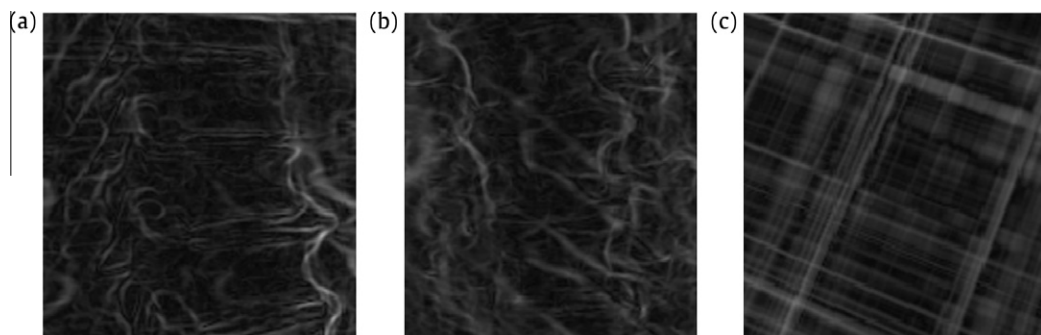


Fig. 7. Lateral (a), coronal (b), and axial (c) cross-sections of a coarsely reconstructed 3D gradient field using two X-rays from the publicly available spine phantom image data (van de Kraats et al., 2005a).

(XMR) has opened up new strategies for registering 3D and 2D images with the goal of augmenting a recently acquired MR image with live X-ray images (Rhode et al., 2003, 2005; Miquel et al., 2006). These registrations are based on carefully pre-calibrated imaging devices and establishment of the position of the operation table with respect to the imaging device during image acquisition. The system requires tracking of different moving components of the XMR system: X-ray C-arm, X-ray table and the sliding MR table top. The X-ray C-arm and the X-ray table are tracked by an optical tracking device using infrared emitting diodes attached to both the C-arm and the X-ray table, while the sliding table is tracked by the MR system software while docked to the MR scanner. It becomes part of the X-ray table when docked to the X-ray system and is then tracked by the optical tracking device. Since the position of patient anatomy relative to the operation table has to be fixed during both image acquisitions, this type of registration requires proper patient immobilization and short times between image acquisitions. The calibration-based 3D/2D registration approach was also proposed for integrating CT and DSA images as part of a multifunctional image-guided therapy suite (MIGTS) that is enabled by the use of a prototype system called the advanced workplace for image-guided surgery (AWIGS, Maquet, Rastatt, Germany) (Jacob et al., 2007; Brandenberger et al., 2007). However, apart from the basic setup, we were not able to find any further studies providing more information about the calibration-based CT to DSA registration or its performance.

3.4. Geometric transformation

According to the nature of spatial transformation and its degrees of freedom, the methods can be classified as *rigid* and *non-rigid*. Because 3D/2D registration is by itself difficult, the majority of published registration methods employed a rigid transformation model, composed of three translations and three rotations. Rigid registration is generally applied when it is assumed that the targeted anatomy fulfills the criterion of rigidity and spatial distortions are not introduced in the image acquisition process or are subsequently corrected. Non-rigid registration is required when the imaged anatomy non-rigidly deforms between acquisitions. In contrast to the large number of rigid 3D/2D registration publications, only a small number of non-rigid methods have been published. The most widespread approach for non-rigid 3D/2D registration is based on 3D shape reconstruction of the anatomy of interest from a small number of X-ray projection images (Benameur et al., 2005a,b, 2003; Fleute and Lavalée, 1999; Tang and Ellis, 2005; Zheng et al., 2006a; Yao and Taylor, 2003; Hurvitz and Joskowicz, 2008; Zheng et al., 2007; Lamecker et al., 2006; Sadowsky et al., 2006, 2007). In these studies, the applied transformations were limited to the transformations allowed by statistical shape models obtained from a larger number of 3D images with principal component analysis. Alternative approaches include the use of a 3D vessel model and a-priori length preservation and smoothness constraints to achieve meaningful non-rigid deformation (Zikic et al., 2008), integration of the algebraic reconstruction technique into a variational registration framework (Prümmer et al., 2006) or a registration framework using support vector regression with free form deformation (Qi et al., 2008). Furthermore, a DRR-based non-rigid 3D/2D registration was also proposed for fiducial-less tracking in radiotherapy where the transformation parameters were determined by generating a full motion field that accounts for non-rigid motions and deformations (Fu and Kuduvali, 2008a). The full 3D motion field was derived from many local 2D motion fields, using multi-level block matching and a similarity measure based on pattern intensity.

3.5. User interaction

While research activities make every effort to develop fully automated 3D/2D registration algorithms (Zheng et al., 2007), some user interaction is usually still needed at least for the final verification of the results. According to the required user interaction, the methods can be *interactive*, *semi-automatic* or *automatic*. Fully *automatic* registration algorithms require that the user provides only the data. Contrary to automatic registration, interactive registration is performed entirely by the user using software tools which provide visual feedback of the current transformation (Gilhuijs et al., 1996a; Remeijer et al., 2000). Unfortunately, accurate interactive registration is time consuming and depends on the skills of the human operator. Most often the level of user interaction is somewhere between these two extremes. For *semi-automatic* registration it is essential that the user provides some initialization to the algorithm, such as segmentation, or steers the algorithm by accepting or rejecting the current registration result. Most of the intrinsic 3D/2D registration methods are semi-automatic and require different levels of user interaction mostly to initialize the registration and/or visually validate the results. The choice of the initialization approach primarily depends on the data available, the application, and the object of registration. Furthermore, the initialization procedure must achieve a registration that is within the capture range of a specific intrinsic 3D/2D registration method, i.e. the maximum displacement from which the registration algorithm is able to recover an accurate result. Registration can be initialized by any of the following approaches:

1. *Clinical setup*: The knowledge of patient position and imaging parameters can be used to put bounds on the range of transformation parameters and thereby approximately determine the location of the patient in the treatment room (Russakoff et al., 2005a, 2003, 2005b, Rohlfing et al. (2005a,b); Byrne et al., 2004; Kerrien et al., 1999; Chelikani et al., 2006; Lemieux et al., 1994). To improve patient positioning even further, immobilization masks (Russakoff et al., 2005a,b, 2003; Chelikani et al., 2006; Jin et al., 2006) and laser positioning with respect to skin tattoos (Clippe et al., 2003; Gilhuijs et al., 1996a; Kim et al., 2001; Jin et al., 2006) were used.
2. *Skin markers*: Placing markers on the patient's skin and their localization is another means of initialization (Turgeon et al., 2005; Clippe et al., 2003; Knaan and Joskowicz, 2003), although the approach may suffer from registration inaccuracy due to skin and patient motion.
3. *Registration of corresponding pairs of anatomical landmarks*: Anatomical landmarks can be manually determined in pre-interventional and intra-interventional images. The position of the patient is then recovered by registration using the closed form solution (Roth et al., 1999; Benameur et al., 2003, 2005b; Hurvitz and Joskowicz, 2008; Zheng et al., 2006a; Zhang et al., 2006).
4. *Manual initialization on images*: With respect to the application and object of registration, manual initialization on images can be achieved in a number of ways. The most generic approach is the use of a graphical user interface (GUI) for exploring the transformation parameter space to achieve the best possible registration as visually assessed by the user (Kaptein et al., 2003; Hipwell et al., 2003; Jaramaz and Eckman, 2006; Vermandel et al., 2006; Yamazaki et al., 2004; You et al., 2001; LaRose, 2001, 2000b; Mahfouz et al., 2003; Roth et al., 1999; Lemieux et al., 1994; Penney et al., 2001; Fukuoka and Hoshino, 1999). Minimal user interaction may also be required by intensity-based 3D/2D registration algorithms where the registration is commonly

restricted to a region of interest (ROI) defined either as a simple rectangle or a bounding contour.⁹ More application specific approaches include setting a seed point for region growing algorithms (Bullitt et al., 1999; Groher et al., 2007b,a; Vermandel et al., 2006; Zikic et al., 2008) or establishing corresponding 3D and 2D vessel skeletons (Bullitt et al., 1999; Liu et al., 1998) in case of vascular applications. In orthopaedic knee kinematic studies each bone of the knee joint was segmented by user interaction and registered separately (Banks and Hodge, 1996; Dennis et al., 2005; Fregly et al., 2005; Hoff et al., 1998; Kaptein et al., 2003; Tang et al., 2004b,a; You et al., 2001; Zuffi et al., 1999; Yamazaki et al., 2004; Mahfouz et al., 2003).

In feature-based methods user interaction may be needed to perform and/or correct segmentation of the 3D and 2D images¹⁰ and/or to remove outliers (spurious edges) (Kaptein et al., 2003; Zuffi et al., 1999; Yamazaki et al., 2004). Since 3D/2D registration is by its nature an ill-defined problem, 3D/2D registration algorithms may provide results that are false. To avoid the risk of guiding a medical intervention by false registration results, the 3D/2D registration should be steered and/or the results validated by the user. The validation of registration results may be supported by proper visualization such as superimposing the contours of a 3D surface (Feldmar et al., 1997; Guezic et al., 2000; Hipwell et al., 2003; Jomier et al., 2006; Groher et al., 2007b,a; Zikic et al., 2008; Liu et al., 1998) or edges extracted from DRRs (Gilhuijs et al., 1996b; Khamene et al., 2006; Livyatan et al., 2003) onto 2D projection images. When a mis-registration is identified, the user can intervene and restart the algorithm from a different starting position to enable a correct registration (Gilhuijs et al., 1996b; Mahfouz et al., 2003).

3.6. Optimization procedure

By its definition, image registration is concerned with finding a geometric transformation that brings one image into the best possible spatial correspondence with another image or physical space by optimizing a registration criterion. The parameters that describe a geometric transformation can be computed *directly* or *searched for*. Direct computation of transformation parameters is possible only when registering 2D or 3D points with known correspondences as in extrinsic and landmark based methods (Section 3.3). In such cases, a simple analytical, closed form solution for point-based rigid registration is available (Horn, 1987; Arun et al., 1987; Umeyama, 1991; Murphy, 2002). In intrinsic registrations such point pairs are not available. Therefore, in feature-based registration methods, parameters have to be searched for iteratively by minimizing the distance between corresponding feature sets. As described in Section 3.3, the registration is performed following an ICP-like approach by alternating the estimation of correspondence and transformation between the geometrical entities extracted from the 3D and 2D images. The original ICP framework

of minimization of the alignment error in the least square sense can be implemented (Chen et al., 2006; Feldmar et al., 1997; Kaptein et al., 2003; Kita et al., 1998; Wunsch and Hirzinger, 1996) or the problem can be cast as a minimization of a cost (energy) function based on the sum of (squared) distances possibly extended by outlier removal procedures, directional information, or regularization terms in case of non-rigid registration.¹¹ Levenberg–Marquardt (Guezic et al., 1998, 2000; Brunie et al., 1993; Lavallee and Szeliski, 1995; Zuffi et al., 1999; Yamazaki et al., 2004), downhill simplex (Fleute and Lavallee, 1999; Groher et al., 2007b,a; Fukuoka and Hoshino, 1999) and gradient descent (Lamecker et al., 2006; Zikic et al., 2008; Benameur et al., 2003; Sundar et al., 2006) were the most commonly used optimization procedures. More recently, local perturbation of the starting position (Guezic et al., 2000; Benameur et al., 2003) and global optimization approaches like exploration/selection (Benameur et al., 2005a,b) or sequential Monte Carlo technique (Florin et al., 2005) were proposed. An alternative approach in feature-based 3D/2D registration is the *library-based* optimization (Banks and Hodge, 1996; Hoff et al., 1998; Cyr et al., 2000; Hermans et al., 2007a) (see Section 3.3).

In the case of intensity-based and gradient-based methods the registration criterion is formulated as a similarity measure defined in the multidimensional space of searched parameters. It is desired that the similarity measure is well-behaved, i.e. is monotone and quasi-convex in the vicinity of the true registered position. This enables the use of local iterative optimization techniques such as the Powell's method,¹² the downhill simplex method,¹³ the gradient descent method (Fu and Kuduvali, 2008b; Hipwell et al., 2003; Khamene et al., 2006; Kim et al., 2005; Munbodh et al., 2006, 2007; Penney et al., 1998, 2001, 2007; Zöllei et al., 2001; Bansal et al., 1999, 2003; Chelikani et al., 2006; Hurvitz and Joskowicz, 2008), the best neighbor search method (Russakoff et al., 2003, 2005a,b; Kubias et al., 2007; Wein et al., 2005) or the hill climbing method (Liao et al., 2006; Rohlfing et al., 2005a). Some of these approaches (Powell's, gradient descent and best neighbor) were recently evaluated in a radiotherapy application (Khamene et al., 2006) and were found to have approximately equal performance. However, to enable registration when the initial position is not close to the correct alignment and to avoid possible local extremes, global optimization approaches and heuristic search strategies were also used to bring the registration parameters within the capturing range of local optimization methods. Different approaches were implemented: simulated annealing (Mahfouz et al., 2003; Dennis et al., 2005; Mahfouz et al., 2005; Vermandel et al., 2006; Zöllei et al., 2001), sampling of parameter space (Jans et al., 2006; Lemieux et al., 1994; Birkfellner et al., 2003; Penney et al., 1998; Munbodh et al., 2009), Monte Carlo random sampling (Dey and Napel, 2006), genetic search (Knaan and Joskowicz, 2003), unscented Kalman Filter (Gong et al., 2006), the pattern search algorithm (Hurvitz and Joskowicz, 2008), multistart strategies (You et al., 2001; Turgeon et al., 2005) and others. However, while these strategies may increase the convergence, their diversity is a testament of how problem-specific they are. A more straightforward and established

⁹ Byrne et al. (2004), Aouadi and Sarry (2008), de Bruin et al. (2008), Benameur et al. (2005a), Chan et al. (2004), Dey and Napel (2006), Fu and Kuduvali (2008b), Göcke et al. (1999), Ho et al. (2007), Imamura et al. (2002), Jans et al. (2006), Khamene et al. (2006), Knaan and Joskowicz (2003), Munbodh et al. (2006, 2008, 2009), Markelj et al. (2007), Nakajima et al. (2002), Penney et al. (1998, 2001, 2007), Hipwell et al. (2003), Rohlfing et al. (2004, 2005b), Roth et al. (1999), Russakoff et al. (2003, 2005a,b), Škerl et al. (2006), Tomažević et al. (2006), Weese et al. (1997a), Zhang et al. (2006), Markelj et al. (2008).

¹⁰ Banks and Hodge (1996), Hoff et al. (1998), Kaptein et al. (2003), You et al. (2001), Zuffi et al. (1999), Yamazaki et al. (2004), Lavallee and Szeliski (1995), Alperin et al. (1994), Bullitt et al. (1999), Feldmar et al. (1997), Florin et al. (2005), Kita et al. (1998), Dennis et al. (2005), Turgeon et al. (2005), Brunie et al. (1993), Fleute and Lavallee (1999), Guezic et al. (1998), Guezic et al. (2000), Wunsch and Hirzinger (1996), Lamecker et al. (2006), Gilhuijs et al. (1996b), Fukuoka and Hoshino (1999), Sadowsky et al. (2006).

¹¹ Bullitt et al. (1999), Liu et al. (1998), Fleute and Lavallee (1999), Groher et al. (2007b,a), Guezic et al. (1998, 2000), Brunie et al. (1993), Lavallee and Szeliski (1995), Zuffi et al. (1999), Yamazaki et al. (2004), Benameur et al. (2003, 2005a,b), Kaptein et al. (2003), Lamecker et al. (2006), Zikic et al. (2008), Alperin et al. (1994), Fregly et al. (2005), Murphy (1997, 1999), Florin et al. (2005), Sundar et al. (2006).

¹² Clippe et al. (2003), Gottesfeld Brown and Bould (1996), Nakajima et al. (2002, 2007), Rohlfing et al. (2005b), Sarrut and Clippe (2001), Birkfellner et al. (2003), Dey and Napel (2006), Khamene et al. (2006), Lemieux et al. (1994), Tomažević et al. (2003, 2006), Markelj et al. (2008), Chan et al. (2004), Chung et al. (2002), van de Kraats et al. (2005b).

¹³ Birkfellner et al. (2009), de Bruin et al. (2008), Chen et al. (2007b), Kim et al. (2001, 2007), Knaan and Joskowicz (2003), Penney et al. (2007), Tang et al. (2004b), You et al. (2001), Livyatan et al. (2003), Tang and Ellis (2005), Turgeon et al. (2005), Dong et al. (2008), Sadowsky et al. (2006, 2007).

approach to avoid false local optima, increase the convergence range, and speed up the registration is the use of a hierarchical multi-resolution¹⁴ and/or a multi-scale (Aouadi and Sarry, 2008; Rohlfing et al., 2005a,b; Russakoff et al., 2003, 2005a,b; Kubias et al., 2007; Munbodh et al., 2009) search strategy. Nevertheless, such strategies are not suitable for all image data. Since down-sampling and/or blurring of image data may suppress some image features and make other non-corresponding image features more similar, the risk of trapping the optimization in a local optimum may be increased. Therefore, as also evident from the literature, these approaches are suitable for registration of image data with a single dominant anatomical structure like the head or large bones, or when models of the anatomical structures obtained by segmentation are used.

3.7. Subject of registration

According to the subject, 3D/2D registrations can be divided into *intrasubject* and *atlas* registrations. Intrasubject registration is performed between images of the same patient. This type of 3D/2D registration is most common, since registration between 3D and 2D images is usually used to establish the position of 3D imaged anatomy of the patient in the coordinate system of the treatment room. When 3D imaging is not possible, 3D/2D registration of an atlas to a limited number of X-ray projection images may be used to obtain a patient-specific 3D shape reconstruction of the anatomy of interest (Benameur et al., 2005a,b, 2003; Fleute and Lavallee, 1999; Tang and Ellis, 2005; Zheng et al., 2006a; Yao and Taylor, 2003; Lamecker et al., 2006; Hurvitz and Joskowicz, 2008; Zheng et al., 2007; Sadowsky et al., 2006, 2007).

3.8. Object of registration and applications

The anatomical structures, to which the reviewed 3D/2D registrations were most frequently applied were:

- head (brain, skull),
- spine and vertebrae,
- limbs (general, femur, tibia, patella, knee joint, hip joint),
- pelvis (entire, perineum) and
- thorax (entire, heart, ribs).

The most frequent applications of 3D/2D registration methods in the reviewed literature were the following:

- radiotherapy (patient positioning, patient motion tracking),
- radiosurgery (arteriovenous malformation),
- orthopedic surgery (total hip replacement, knee replacement, total hip arthroplasty),
- interventional neuroradiology (head, neck, and spine minimally invasive procedures),
- vascular interventional radiology (angioplasty, shunt, embolization),
- kinematic analysis (knee kinematics), etc.

The interventions that currently most benefit from 3D/2D image registration are radiotherapy and radiosurgery, where as a result of the research efforts two commercial systems, Accuray Cyberknife (Adler et al., 1999; Fu and Kuduvali, 2008b; Fu and

Kuduvali, 2008a) and BrainLab Novalis (Agazaryan et al., 2008), were developed, both of which are DRR-based. In radiotherapy, it is crucial that the treated anatomy is accurately aligned with radiation beams. Intrinsic 3D/2D registration can be used for treatment of tumors near bony reference structures like tumor of the brain since it can be expected that the relation between brain and skull is almost rigid (Adler et al., 1999; Chen et al., 2006, 2008; Fu and Kuduvali, 2008b; Ho et al., 2007; Jin et al., 2006; Khamene et al., 2006; Gilhuijs et al., 1996b; Murphy, 1997, 1999; Sirois et al., 1999; LaRose, 2001; Romanelli et al., 2006a). In spinal radiosurgery the individual vertebrae were rigidly registered (Adler et al., 1999; Ho et al., 2007; Fu and Kuduvali, 2008b; Jans et al., 2006; Russakoff et al., 2005a; Rohlfing et al., 2005a) or the vertebral structures were used as reference points for non-rigid registration (Fu and Kuduvali, 2008a). For alignment and tracking of the prostate, intrinsic 3D/2D registration of the pelvis as a reference structure was used (Chelikani et al., 2006; Munbodh et al., 2006, 2008, 2007, 2009; Remeijer et al., 2000; Jans et al., 2006; Bansal et al., 1999, 2003; Clippe et al., 2003; Chen et al., 2008). However, since the prostate can move with respect to the pelvis, the registration of extrinsic markers implanted in the prostate has become the clinical method of choice (Aubry et al., 2004; Litzenberg et al., 2002; Mu et al., 2008). The marker point-based approach (Mu et al., 2008) was used for treating tumors in the liver (Choi et al., 2005), lung (Christie et al., 2005; Shirato et al., 2000; Schweikard et al., 2004) and pancreas (Goodman and Koong, 2005), because registration based on nearby bony structures was not accurate enough. For treating and tracking lung tumors a 2D/2D registration of pre-calculated to inter-interventional DRRs of the rib cage in combination with an optical tracker was proposed by Schweikard et al. (2005).

Many current orthopedic procedures require 3D planning from pre-interventional CT or MR images, while X-ray imaging is usually used for guidance. In spine surgery, pedicle screw placement and cement reinforcement of vertebra are the most frequent applications of 3D/2D image registration. Since spine is an articulated structure, registration was based on rigid registration of a single vertebra (Livyatan et al., 2003; Penney et al., 2001; Tomažević et al., 2006; Markelj et al., 2008; Tomažević et al., 2003; van de Kraats et al., 2005b; Weese et al., 1997b; Zhang et al., 2006; Jonic et al., 2003; Hamadeh et al., 1998; Russakoff et al., 2003). The 3D/2D registration can also improve the total hip replacement procedure. Registration of CT and X-ray images of the femur was used for positioning of the femoral implant (Gueziec et al., 1998, 2000; Hurvitz and Joskowicz, 2008; Zheng et al., 2007) and enabled analysis of cup positioning (Jaramaz and Eckman, 2006; Penney et al., 2007; LaRose et al., 2000b). 3D/2D registration of CT to a single fluoroscopic image was used in tracking of the proximal bone fragment in femoral fracture reduction surgery (Nakajima et al., 2007). 3D/2D image registration of knee bones and knee implants was used to analyze knee kinematics before (Dennis et al., 2005; Fregly et al., 2005; Tang et al., 2004b; You et al., 2001) and after (Banks and Hodge, 1996; Hoff et al., 1998; Kaptein et al., 2003; Mahfouz et al., 2003; Yamazaki et al., 2004; Zuffi et al., 1999; Hermans et al., 2007a; Fukuoka and Hoshino, 1999) a total knee arthroplasty procedure. Orthopedic diagnostics may also benefit from 3D analysis of 2D images. 3D/2D registration was used for measuring the 3D curvature of scoliotic spine (Benameur et al., 2005b) and 3D reconstruction and classification of the scoliotic rib cage from biplanar X-ray images (Benameur et al., 2005a).

Interventional neuroradiology and vascular interventional radiology are concerned with performing minimally invasive procedures by maneuvering through blood vessels using image guidance to reach the treatment site. The former is concerned with diagnosis and treatment of the head, neck, and spine pathology, while the latter is concerned with interventions elsewhere in the

¹⁴ Benameur et al. (2005b), Birkfellner et al. (2003), Byrne et al. (2004), Chen et al. (2008), Chung et al. (2002), Dey and Napel (2006), Fu and Kuduvali (2008b,a), Gueziec et al. (1998, 2000), Hipwell et al. (2003), Ho et al. (2007), Imamura et al. (2002), Jonic et al. (2003), Kerrien et al. (1999), Khamene et al. (2006), Knaan and Joskowicz (2003), Lavallee and Szeliski (1995), Lemieux et al. (1994), Munbodh et al. (2006, 2008, 2007, 2009), Penney et al. (2001, 2007), Tang et al. (2004b), Zhang et al. (2006), Zheng et al. (2006b, 2008), Zöllei et al. (2001), Kubias et al. (2007), Lamecker et al. (2006), Cyr et al. (2000).

body. In these procedures, a clinician follows the path of the catheter in the patient's body with the help of dynamic intra-interventional 2D X-ray imaging. For the purpose of diagnosis and planning, 3D CT or MR angiographic images may also be acquired prior to treatment. To provide 2D and 3D images with high contrast vessel structures, an opaque contrast material has to be injected into the patient just before imaging. Due to the complex 3D structure of vessel trees, catheter navigation supported by 2D imaging is not trivial. Navigation can be improved by 3D/2D registration. By incorporating 3D/2D registration the "road map" obtained from 3D images may be projected and visualized on dynamic 2D X-ray images or the position of the catheter detected on 2D X-ray images may be visualized on pre-interventional 3D images. The support of 3D/2D registration was proposed for neuro,¹⁵ cardiac (Imamura et al., 2002; Turgeon et al., 2005; Chen et al., 2007b) and liver (Groher et al., 2007a,b; Jomier et al., 2006; Zikic et al., 2008) interventions. We are not aware of any publications on intrinsic 3D/2D image registrations applied to non-vascular interventional radiology, e.g. tissue ablation. This is probably due to demanding challenges that have to be addressed in these applications, in particular the patient and respiratory motion that is present during such procedures and the real-time requirements of continuous guidance of the tool. Therefore, to satisfy these constraints, point-based marker registration is still preferred, as described in a very recent publication (Nicolau et al., 2009).

In addition to publications that focus on one or more specific medical applications a large volume of work is concerned with generally applicable registration methods, overviews/evaluations of a specific aspect of 3D/2D registration or ground truth registration. Generally applicable registration methods propose new 3D/2D registration approaches.¹⁶ Several publications focus on speeding up DRR-based methods (Birkfellner et al., 2003, 2005a,b; Rohlfing et al., 2005b; Russakoff et al., 2005b; Weese et al., 1999; Kubias et al., 2007; Cyr et al., 2000; Wein et al., 2005) and on comparison/development of similarity measures (Birkfellner et al., 2009; Munbodh et al., 2009; Kim et al., 2007; Penney et al., 1998; Škerl et al., 2006; Zheng, 2008; Zheng et al., 2006b; Clippe et al., 2003; Hipwell et al., 2003). Several specific aspects of 3D/2D registration were also evaluated like preprocessing of images (Kim et al., 2005; Mahfouz et al., 2005; Nakajima et al., 2002; Jans et al., 2006) and the impact of X-ray views used for registration (Tomažević et al., 2007; Yao and Taylor, 2003; Khamene et al., 2006; Sadowsky, 2007). Finally, three publicly available gold standard evaluation methodologies were published (Tomažević et al., 2004; van de Kraats et al., 2005a; Pawiro et al., 2010).

4. Evaluation of 3D/2D registration methods

As in any other discipline of medical image processing, evaluation has become an integral part of peer-reviewed publications on 3D/2D registration. Evaluation is paramount as it allows to determine the performance and limitations of a proposed method. Furthermore, evaluation also clarifies the potential clinical applications and added value of a method (Jannin et al., 2002). A prerequisite for evaluation of (3D/2D) image registration is

standardization of evaluation methodology which includes: design of evaluation image data sets, definition of corresponding ground truth and its accuracy, selection of evaluation criteria, design of evaluation metrics and finally design of the evaluation protocol (Jannin et al., 2002, 2006a,b). Furthermore, the evaluation methodology also determines the evaluation objective (Jannin et al., 2006a), which describes the clinical context and the clinical objective of the evaluation study. According to the evaluation protocol, a given evaluation image data set and input parameters are used in the registration experiment. The output of the image registration method is then compared to the ground truth registration using the evaluation metric, which gives a measure of the quality of registration in reference to the ground truth. Finally, the obtained quality indices may be used for statistical analysis of the results and hypothesis testing. Thereby, it can be determined if the proposed registration meets the expected requirements. In addition, it is also critical that the standardized evaluation methodology is freely available to enable objective and unbiased comparison between methods proposed by different authors.

The guidelines for creating a standardized evaluation methodology and conducting a reference-based evaluation study were proposed by Jannin et al. (2006a). To the best of our knowledge, only three 3D/2D registration evaluation methodologies that followed these guidelines are publicly available. Tomažević et al. (2004)¹⁷ used a section of cadaveric lumbar spine comprising vertebrae L1–L5 with intervertebral disks and several millimeters of soft tissue and acquired CT, MR and 18 X-ray images separated by 20° rotation around the axial axis. Similarly, image data in the standardized evaluation methodology proposed by van de Kraats et al. (2005a)¹⁸ consists of 2D fluoroscopic X-ray images and 3D CT, MR and 3D rotational X-ray images of two defrosted segments of a spinal column. The gold standard registrations in the first methodology were obtained by rigid 3D/3D registration of fiducial marker points in CT and MR to marker points reconstructed from X-ray images, while the second methodology used a mutual information-based rigid registration of CT and MR images to corresponding 3D rotational X-ray images (Maes et al., 1997). Most recently, a third standardized evaluation based on a fresh porcine cadaver head was proposed (Pawiro et al., 2010). The evaluation methodology image data set features CBCT, CT, MR-T1, MR-T2, and MR-PD 3D images, and lateral and anterior posterior kV and MV 2D X-ray images. The gold standard registrations were obtained by using suitable fiducial markers attached to the skull of the pig. The most significant advantage of the latter methodology over the two previously presented, is that all soft tissue is presented, which much better reflects a realistic clinical situation.

Despite of the three publicly available evaluation methodologies the authors of new 3D/2D registration methods still most often evaluate their methods on simulated images only or on their, publicly unavailable, image data sets with an often unclear evaluation methodology and metrics that do not allow a direct comparison to other published results. This has to be attributed somewhat to the fact that evaluation methodologies are application specific and that publications (Tomažević et al., 2004; van de Kraats et al., 2005a; Pawiro et al., 2010) are rather recent. However, at least for 3D/2D registrations which are not aimed at a specific application, the use of publicly available standardized evaluation methodologies should/must become a standard approach of performance assessment.

¹⁵ Alperin et al. (1994), Bullitt et al. (1999), Byrne et al. (2004), Chan et al. (2004), Chung et al. (2002), Florin et al. (2005), Hipwell et al. (2003), Kita et al. (1998), Kerrien et al. (1999), McLaughlin et al. (2005), Vermandel et al. (2006), Groher et al. (2007b), Liu et al. (1998), Sundar et al. (2006).

¹⁶ Aouadi and Sarry (2008), Brunie et al. (1993), Dey and Napel (2006), Feldmar et al. (1997), Gong et al. (2006), Gottesfeld Brown and Boulton (1996), Lamecker et al. (2006), Lavalée and Szeliski (1995), Lemieux et al. (1994), Liao et al. (2006), Prümmer et al. (2006), Rohlfing and Maurer (2002), Roth et al. (1999), Fleute and Lavalée (1999), Tang and Ellis (2005), Wunsch and Hirzinger (1996), Zöllei et al. (2001), Dong et al. (2008), Hurvitz and Joskowicz (2008), Qi et al. (2008), Wein et al. (2005).

¹⁷ <http://lit.fe.uni-lj.si/tools.php>.

¹⁸ <http://www.isi.uu.nl/Research/Databases/GS/>.

5. Conclusion

An overview of 3D/2D data registration methods that utilize 3D pre-interventional CT or MR images and 2D intra-interventional X-ray projection images has been presented. The publications were surveyed according to the classification proposed by Maintz and Viergever (1998). Using such a classification several aspects of 3D/2D registration were examined.

As could be expected, the review of relevant literature did not put forth any group of methods as clearly superior to others. Rather, the choice of a particular method depends on the application. While feature-based methods dominate where reliable and straightforward segmentation can be used to determine edges and surfaces of anatomical structures or structures of interest, i.e. orthopedics, the intensity-based methods are more common in applications where anatomical structures are not as distinctive and therefore, all image information should be used to achieve registration. Gradient-based methods seem to fit in between the two extremes by taking advantage of geometrical as well as intensity information and as such seem promising in a variety of applications.

The review revealed that the field of 3D/2D registration is dominated by DRR-based methods. The research efforts culminated in the development of two commercial IGI treatment suites using 3D/2D DRR-based registration for radiotherapy and radiosurgery (Accuray Cyberknife, Brainlab Novalis). Thereby, with the introduction into every day clinical practice the 3D/2D registration reached an important milestone and became an established image processing technique. At the same time, 3D imaging devices like kV and MV CBCT were introduced into the radiation therapy room enabling 3D/3D pre- to intra-interventional image registration. With these technological advances the initially set problem of bringing the high-quality 3D images into the intervention room seems to be solved to a degree sufficient for clinical implementation. Therefore, new research challenges for 3D/2D registration have to be identified and addressed. The most obvious is the extension of rigid registration approaches to non-rigid which has numerous clinical applications, e.g. correction of soft tissue deformations during an intervention. Furthermore, the existing methods need to be improved to enable tracking of the clinical target with rigid or even non-rigid 3D/2D registration e.g. dynamic tumor motion monitoring during radiotherapy (Choi et al., 2005; Christie et al., 2005; Shirato et al., 2000; Goodman and Koong, 2005; Gendrin et al., 2009). But, perhaps the most important issue of all is a continuous effort on the part of the researchers as well as clinicians to work together in bringing the 3D/2D registration technology into the clinical theater.

Acknowledgment

The authors are grateful to J. Spoerk and W. Birkfellner, Center for Biomedical Engineering and Physics, Medical University Vienna, for providing the DRR images. This work was supported by the Ministry of Higher Education, Science and Technology, Republic of Slovenia under the Grants P2-0232, L2-7381, L2-9758, Z2-9366, J2-0716, L2-2023 and J7-2246.

References

Adler, J.R., Murphy, M.J., Chang, S.D., Hancock, S.L., 1999. Image-guided robotic radiosurgery. *Neurosurgery* 44 (6), 1299–1306.

Agazaryan, N., Tenn, S.E., Desalles, A.A.F., Selch, M.T., 2008. Image-guided radiosurgery for spinal tumors: methods, accuracy and patient intrafraction motion. *Phys. Med. Biol.* 53 (6), 1715–1727.

Aird, E.G.A., Conway, J., 2002. CT simulation for radiotherapy treatment planning. *Brit. J. Radiol.* 75 (900), 937–949.

Alperin, N., Levin, D.N., Pelizzari, C.A., 1994. Retrospective registration of X-ray angiograms with MR images by using vessels as intrinsic landmarks. *J. Magn. Reson. Imag.* 4 (2), 139–144.

Aouadi, S., Sarry, L., 2008. Accurate and precise 2D–3D registration based on X-ray intensity. *Comput. Vis. Image Und.* 110 (1), 134–151.

Arun, K.S., Huang, T.S., Blostein, S.D., 1987. Least-squares fitting of 2 3-D point sets. *IEEE Trans. Pattern Anal. Mach. Intell.* 9 (5), 699–700.

Aubry, J.F., Beaulieu, L., Girouard, L.M., Aubin, S., Tremblay, D., Laverdiere, J., Vigneault, E., 2004. Measurements of intrafraction motion and interfraction and intrafraction rotation of prostate by three-dimensional analysis of daily portal imaging with radiopaque markers. *Int. J. Radiat. Oncol. Biol. Phys.* 60 (1), 30–39.

Audette, M.A., Siddiqi, K., Ferrie, F.P., Peters, T.M., 2003. An integrated range-sensing, segmentation and registration framework for the characterization of intra-surgical brain deformations in image-guided surgery. *Comput. Vis. Image Und.* 89 (2–3), 226–251.

Avanzo, M., Romanelli, P., 2009. Spinal radiosurgery: technology and clinical outcomes. *Neurosurg. Rev.* 32 (1), 1–12.

Bale, R.J., Burtcher, J., Eisner, W., Obwegeser, A.A., Rieger, M., Sweeney, R.A., Dessl, A., Giacomuzzi, S.M., Twerdy, K., Jaschke, W., 2000. Computer-assisted neurosurgery by using a noninvasive vacuum-affixed dental cast that acts as a reference base: another step toward a unified approach in the treatment of brain tumors. *J. Neurosurg.* 93 (2), 208–213.

Banks, S.A., Hodge, W.A., 1996. Accurate measurement of three-dimensional knee replacement kinematics using single-plane fluoroscopy. *IEEE Trans. Biomed. Eng.* 43 (6), 638–649.

Bansal, R., Staib, L.H., Chen, Z., Rangarajan, A., Knisely, J., Nath, R., Duncan, J.S., 1999. A minimax entropy registration framework for patient setup verification in radiotherapy. *Comput. Aided Surg.* 4 (6), 287–304.

Bansal, R., Staib, L.H., Chen, Z., Rangarajan, A., Knisely, J., Nath, R., Duncan, J.S., 2003. Entropy-based dual-portal-to-3-DCT registration incorporating pixel correlation. *IEEE Trans. Med. Imag.* 22 (1), 29–49.

Benamer, S., Mignotte, M., Parent, S., Labelle, H., Skalli, W., De Guise, J., 2003. 3D/2D registration and segmentation of scoliotic vertebrae using statistical models. *Comput. Med. Imag. Graph.* 27 (5), 321–337.

Benamer, S., Mignotte, M., Destrempe, F., De Guise, J.A., 2005a. Three-dimensional biplanar reconstruction of scoliotic rib cage using the estimation of a mixture of probabilistic prior models. *IEEE Trans. Biomed. Eng.* 52 (10), 1713–1728.

Benamer, S., Mignotte, M., Labelle, H., De Guise, J.A., 2005b. A hierarchical statistical modeling approach for the unsupervised 3-D biplanar reconstruction of the scoliotic spine. *IEEE Trans. Biomed. Eng.* 52 (12), 2041–2057.

Besl, P.J., McKay, N.D., 1992. A method for registration of 3-D shapes. *IEEE Trans. Pattern Anal. Mach. Intell.* 14 (2), 239–256.

Bijhold, J., 1993. Three-dimensional verification of patient placement during radiotherapy using portal images. *Med. Phys.* 20 (2), 347–356.

Birkfellner, W., Wirth, J., Burgstaller, W., Baumann, B., Staedele, H., Hammer, B., Gellrich, N.C., Jacob, A.L., Regazzoni, P., Messmer, P., 2003. A faster method for 3D/2D medical image registration – a simulation study. *Phys. Med. Biol.* 48 (16), 2665–2679.

Birkfellner, W., Seemann, R., Figl, M., Hummel, J., Ede, C., Homolka, P., Yang, X., Niederer, P., Bergmann, H., 2005a. Fast DRR generation for 2D/3D registration. In: Duncan, J.S., Gerig, G. (Eds.), Eighth International Conference on Medical Image Computing and Computer-Assisted Intervention (MICCAI 2005), Part 2, Lecture Notes in Computer Science, vol. 3750. Springer, Palm Springs, CA, USA, pp. 960–967.

Birkfellner, W., Seemann, R., Figl, M., Hummel, J., Ede, C., Homolka, P., Yang, X.H., Niederer, P., Bergmann, H., 2005b. Wobbled splatting – a fast perspective volume rendering method for simulation of X-ray images from CT. *Phys. Med. Biol.* 50 (9), N73–N84.

Birkfellner, W., Figl, M., Kettenbach, J., Hummel, J., Homolka, P., Scherthaner, R., Nau, T., Bergmann, H., 2007. Rigid 2D/3D slice-to-volume registration and its application on fluoroscopic CT images. *Med. Phys.* 34 (1), 246–255.

Birkfellner, W., Stock, M., Figl, M., Gendrin, C., Hummel, J., Dong, S., Kettenbach, J., Georg, D., Bergmann, H., 2009. Stochastic rank correlation: a robust merit function for 2D/3D registration of image data obtained at different energies. *Med. Phys.* 36 (8), 3420–3428.

Brandenberger, D., Birkfellner, W., Baumann, B., Messmer, P., Huegli, R.W., Regazzoni, P., Jacob, A.L., 2007. Positioning accuracy in a registration-free CT-based navigation system. *Phys. Med. Biol.* 52 (23), 7073–7086.

Bricault, I., Ferretti, G., Cinquin, P., 1998. Registration of real and CT-derived virtual bronchoscopic images to assist transbronchial biopsy. *IEEE Trans. Med. Imag.* 17 (5), 703–714.

Brunie, L., Lavalée, S., Troccaz, J., Cinquin, P., Bolla, M., 1993. Pre- and intra-irradiation multimodal image registration: principles and first experiments. *Radiother. Oncol.* 29 (2), 244–252.

Bullitt, E., Liu, A., Aylward, S.R., Coffey, C., Stone, J., Mukherji, S.K., Muller, K.E., Pizer, S.M., 1999. Registration of 3D cerebral vessels with 2D digital angiograms: clinical evaluation. *Acad. Radiol.* 6 (9), 539–546.

Burschka, D., Li, M., Ishii, M., Taylor, R.H., Hager, G.D., 2005. Scale-invariant registration of monocular endoscopic images to CT-scans for sinus surgery. *Med. Image Anal.* 9 (5), 413–426.

Byrne, J.V., Colominas, C., Hipwell, J., Cox, T., Noble, J.A., Penney, G.P., Hawkes, D.J., 2004. Assessment of a technique for 2D–3D registration of cerebral intra-arterial angiography. *Brit. J. Radiol.* 77 (914), 123–128.

Cabral, B., Cam, N., Foran, J., 1994. Accelerated volume rendering and tomographic reconstruction using texture mapping hardware. In: VVS'94: Proceedings of the

- 1994 Symposium on Volume Visualization. ACM Press, New York, NY, USA, pp. 91–98.
- Chan, H.M., Chung, A.C.S., Yu, S., Wells, W.M.I.I.I., 2004. 2D–3D vascular registration between digital subtraction angiographic (DSA) and magnetic resonance angiographic (MRA) images. In: IEEE International Symposium on Biomedical Imaging: Nano to Macro, vol. 1, pp. 708–711.
- Chang, S.D., Main, W., Martin, D.P., Gibbs, I.C., Heilbrun, M.P., 2003. An analysis of the accuracy of the cyberknife: a robotic nameless stereotactic radiosurgical system. *Neurosurgery* 52 (1), 140–146.
- Chelikani, S., Purushothaman, K., Knisely, J., Chen, Z., Nath, R., Bansal, R., Duncan, J., 2006. A gradient feature weighted minimax algorithm for registration of multiple portal images to 3DCT volumes in prostate radiotherapy. *Int. J. Radiat. Oncol. Biol. Phys.* 65 (2), 535–547.
- Chen, X., Varley, M.R., Shark, L.K., Shentall, G.S., Kirby, M.C., 2006. An extension of iterative closest point algorithm for 3D–2D registration for pre-treatment validation in radiotherapy. In: International Conference on Medical Information Visualisation–BioMedical Visualisation (MedVis'06), pp. 3–8.
- Chen, L.L., Nguyen, T.B., Jones, E., Chen, Z.Q., Luo, W., Wang, L., Price, R.A., Pollack, A., Ma, C.M.C., 2007a. Magnetic resonance-based treatment planning for prostate intensity-modulated radiotherapy: creation of digitally reconstructed radiographs. *Int. J. Radiat. Oncol. Biol. Phys.* 68 (3), 903–911.
- Chen, X., Gilkeson, R.C., Feia, B.W., 2007b. Automatic 3D-to-2D registration for CT and dual-energy digital radiography for calcification detection. *Med. Phys.* 34 (12), 4934–4943.
- Chen, X., Varley, M.R., Shark, L.K., Shentall, G.S., Kirby, M.C., 2008. A computationally efficient method for automatic registration of orthogonal X-ray images with volumetric CT data. *Phys. Med. Biol.* 53 (4), 967–983.
- Choi, I.B., Choi, B.O., Jang, H.S., Ryu, M.R., Kang, Y.N., Hahn, S.T., Han, J.Y., Jung, K.W., Bae, S.H., Choi, J.Y., Yoon, S.K., 2005. Cyberknife management of primary hepatocellular carcinoma. In: Mould, R.F., Schulz, R.A. (Eds.), *Robotic Radiosurgery*, vol. 1. Cyberknife Society Press, Sunnyvale, CA, pp. 279–286 (Chapter 25).
- Christie, N.A., Pennathur, A., Luketich, J.D., 2005. Stereotactic radiosurgery for lung tumors. In: Mould, R.F., Schulz, R.A. (Eds.), *Robotic Radiosurgery*, vol. 1. Cyberknife Society Press, Sunnyvale, CA, pp. 269–278 (Chapter 24).
- Chung, A., Wells, W., Norbashi, A., Grimson, W., 2002. Multi-modal image registration by minimising Kullback–Leibler distance. In: Dohi, T., Kikinis, R. (Eds.), *Fifth International Conference on Medical Image Computing and Computer-Assisted Intervention (MICCAI 2002)*, Lecture Notes in Computer Science, vol. 2489. Springer, Tokyo, Japan, pp. 525–532.
- Clippe, S., Sarrut, D., Malet, C., Miguet, S., Ginestet, C., Carrie, C., 2003. Patient setup error measurement using 3D intensity-based image registration techniques. *Int. J. Radiat. Oncol. Biol. Phys.* 56 (1), 259–265.
- Colchester, A.C.F., Zhao, J., Holton-Tainter, K.S., Henri, C.J., Maitland, N., Roberts, P.T.E., Harris, C.G., Evans, R.J., 1996. Development and preliminary evaluation of VISLAN, a surgical planning and guidance system using intra-operative video imaging. *Med. Image Anal.* 1 (1), 73–90.
- Comeau, R.M., Sadiqot, A.F., Fenster, A., Peters, T.M., 2000. Intraoperative ultrasound for guidance and tissue shift correction in image-guided neurosurgery. *Med. Phys.* 27 (4), 787–800.
- Cyr, C., Kamal, A., Sebastian, T., Kimia, B., 2000. 2D–3D registration based on shape matching. In: IEEE Workshop on Mathematical Methods in Biomedical Image Analysis (MMBIA 2000). IEEE Computer Society, Hilton Head Island, SC, USA, pp. 198–203.
- de Bruin, P.W., Kaptein, B.L., Stoel, B.C., Reiber, J.H.C., Rozing, P.M., Valstar, E.R., 2008. Image-based RSA: Roentgen stereophotogrammetric analysis based on 2D–3D image registration. *J. Biomech.* 41 (1), 155–164.
- De Buck, S., Maes, F., Ector, J., Bogaert, J., Dymarkowski, S., Heidbuchel, H., Suetens, P., 2005. An augmented reality system for patient-specific guidance of cardiac catheter ablation procedures. *IEEE Trans. Med. Imag.* 24 (11), 1512–1524.
- Deligianni, F., Chung, A.J., Yang, G.Z., 2004. Patient-specific bronchoscope simulation with pq-space-based 2-D/3-D registration. *Comput. Aided Surg.* 9 (5), 215–226.
- Deligianni, F., Chung, A.J., Yang, G.Z., 2006. Nonrigid 2-D/3-D registration for patient specific bronchoscopy simulation with statistical shape modeling: Phantom validation. *IEEE Trans. Med. Imag.* 25 (11), 1462–1471.
- Dennis, D.A., Mahfouz, M.R., Komistek, R.D., Hoff, W., 2005. In vivo determination of normal and anterior cruciate ligament-deficient knee kinematics. *J. Biomech.* 38 (2), 241–253.
- de Silva, R., Gutierrez, L.F., Raval, A.N., McVeigh, E.R., Ozturk, C., Lederman, R.J., 2006. X-ray fused with magnetic resonance imaging (XFM) to target endomyocardial injections – validation in a swine model of myocardial infarction. *Circulation* 114 (22), 2342–2350.
- Dey, J., Napel, S., 2006. Targeted 2D/3D registration using ray normalization and a hybrid optimizer. *Med. Phys.* 33 (12), 4730–4738.
- Dieterich, S., Rodgers, J., Chan, R., 2008. *Radiosurgery*. In: Peters, T.M., Cleary, K. (Eds.), *Image Guided Interventions Technology and Applications*. Springer, pp. 461–500 (Chapter 16).
- DiMaio, S., Kapur, T., Cleary, K., Aylward, S., Kazanzides, P., Vosburgh, K., Ellis, R., Duncan, J., Farahani, K., Lemke, H., Peters, T., Lorensen, W., Gobbi, D., Haller, J., Clarke, L., Pizer, S., Taylor, R., Galloway Jr., R., Fichtinger, G., Hata, N., Lawson, K., Tempny, C., Kikinis, R., Jolesz, F., 2007. Challenges in image-guided therapy system design. *Neuroimage* 37 (Suppl. 1), S144.
- Dong, S., Kettenbach, J., Hinterleitner, I., Bergmann, H., Birkfellner, W., 2008. The zernike expansion – an example of a merit function for 2D/3D registration based on orthogonal functions. In: Metaxas, D., Axel, L., Fichtinger, G., Székely, G. (Eds.), *11th International Conference on Medical Image Computing and Computer-Assisted Intervention (MICCAI 2008)*, Lecture Notes in Computer Science, vol. 5242. Springer, New York, USA, pp. 964–971.
- Fei, B.W., Duerk, J.L., Boll, D.T., Lewin, J.S., Wilson, D.L., 2003. Slice-to-volume registration and its potential application to interventional MRI-guided radio-frequency thermal ablation of prostate cancer. *IEEE Trans. Med. Imag.* 22 (4), 515–525.
- Feldmar, J., Ayache, N., Betting, F., 1997. 3D–2D projective registration of free-form curves and surfaces. *Comput. Vis. Image Und.* 65 (3), 403–424.
- Fitzpatrick, J.M., West, J.B., 2001. The distribution of target registration error in rigid-body point-based registration. *IEEE Trans. Med. Imag.* 20 (9), 917–927.
- Fitzpatrick, J.M., West, J.B., Maurer, C.R., 1998. Predicting error in rigid-body point-based registration. *IEEE Trans. Med. Imag.* 17 (5), 694–702.
- Fleute, M., Lavalée, S., 1999. Nonrigid 3-D/2-D registration of images using statistical models. In: Taylor, C., Colchester, A. (Eds.), *Second International Conference on Medical Image Computing and Computer-Assisted Intervention (MICCAI'99)*, Lecture Notes in Computer Science, vol. 1679. Springer, Cambridge, UK, pp. 138–147.
- Florin, C., Williams, J., Khamene, A., Paragios, N., 2005. Registration of 3D angiographic and X-ray images using sequential Monte Carlo sampling. In: Liu, Y., Yang, T., Zhang, C. (Eds.), *First International Workshop on Computer Vision for Biomedical Image Applications (CVBIA 2005)*, Lecture Notes in Computer Science, vol. 3765. Springer, Beijing, China, pp. 427–436.
- Fregly, B.J., Rahman, H.A., Banks, S.A., 2005. Theoretical accuracy of model-based shape matching for measuring natural knee kinematics with single-plane fluoroscopy. *J. Biomech. Eng.* 127 (4), 692–699.
- Frühwald, L., Kettenbach, J., Figl, M., Hummel, J., Bergmann, H., Birkfellner, W., 2009. A comparative study on manual and automatic slice-to-volume registration of CT images. *Eur. Radiol.*
- Fu, D., Kuduvalli, G., 2008a. Fiducial-less tracking with non-rigid image registration. US Patent 7327865, Accuray, Inc.
- Fu, D.S., Kuduvalli, G., 2008b. A fast, accurate, and automatic 2D–3D image registration for image-guided cranial radiosurgery. *Med. Phys.* 35 (5), 2180–2194.
- Fukuoka, Y., Hoshino, A.A.I., 1999. A simple radiographic measurement method for polyethylene wear in total knee arthroplasty. *IEEE Trans. Rehabil. Eng.* 7 (2), 228–233.
- Gall, K.P., Thornton, A.F., Munzenrider, J., Rosenthal, S., 1993. Experience using radiopaque fiducial points for patient alignment during radiotherapy. *Int. J. Radiat. Oncol. Biol. Phys.* 27, 161.
- Galloway, R.L., 2001. The process and development of image-guided procedures. *Annu. Rev. Biomed. Eng.* 3, 83–108.
- Galloway, R.L., Maciunas, R.J., 1990. Stereotaxic neurosurgery. *Crit. Rev. Biomed. Eng.* 18 (3), 181–205.
- Gendrin, C., Spoerk, J., Weber, C., Figl, M., Georg, D., Bergmann, H., Birkfellner, W., 2009. 2D/3D registration at 1 Hz using GPU splat rendering. In: Barattieri, C., Frisoni, C., Manset, D. (Eds.), *MICCAI-Grid Workshop, Medical Imaging on Grids, HPC and GPU-based Technologies*. London, UK, pp. 6–14, <<http://www.i3s.unice.fr/FINAL.pdf>>.
- Germano, I., 2000. *Advanced Techniques in Image-Guided Brain and Spine Surgery*. Thieme Medical Publishers.
- Gilhuijs, K.G.A., Drukker, K., Touw, A., van de Ven, P.J.H., van Herk, M., 1996a. Interactive three dimensional inspection of patient setup in radiation therapy using digital portal images and computed tomography data. *Int. J. Radiat. Oncol. Biol. Phys.* 34 (4), 873–885.
- Gilhuijs, K.G.A., van de Ven, P.J.H., van Herk, M., 1996b. Automatic three-dimensional inspection of patient setup in radiation therapy using portal images, simulator images, and computed tomography data. *Med. Phys.* 23 (3), 389–399.
- Göcke, R., Weese, J., Schumann, H., 1999. Fast volume rendering methods for voxel-based 2D/3D registration – a comparative study. In: Pernuš, F., Kováčič, S., Stiehl, H.S., Viergever, M.A. (Eds.), *International workshop on Biomedical Image Registration (WBIR'99)*. Bled, Slovenia, pp. 89–102.
- Goitein, M., Abrams, M., Rowell, D., Pollari, H., Wiles, J., 1983. Multidimensional treatment planning. 2. Beam eye-view, back projection, and projection through CT sections. *Int. J. Radiat. Oncol. Biol. Phys.* 9 (6), 789–797.
- Gong, R.H., Stewart, A.J., Abolmaesumi, P., 2006. A new method for CT to fluoroscopy registration based on unscented Kalman filter. In: Larsen, R., Nielsen, M., Sparring, J. (Eds.), *Ninth International Conference on Medical Image Computing and Computer-Assisted Intervention (MICCAI 2006)*, Part 1, Lecture Notes in Computer Science, vol. 4190. Springer, Copenhagen, Denmark, pp. 891–898.
- Goodman, K.A., Koong, A.C., 2005. Cyberknife radiosurgery for pancreatic cancer. In: Mould, R.F., Schulz, R.A. (Eds.), *Robotic Radiosurgery*, vol. 1. Cyberknife Society Press, Sunnyvale, CA, pp. 287–300 (Chapter 26).
- Gottesfeld Brown, L.M., Boulton, T.E., 1996. Registration of planar film radiographs with computed tomography. In: *Proceedings of the IEEE Workshop on Mathematical Methods in Biomedical Image Analysis*, pp. 42–51.
- Groher, M., Bender, F., Hoffmann, R.-T., Navab, N., 2007a. Segmentation-driven 2D–3D registration for abdominal catheter interventions. In: Ayache, N., Ourselin, S., Maeder, A. (Eds.), *10th International Conference on Medical Image Computing and Computer-Assisted Intervention (MICCAI 2007)*, Lecture Notes in Computer Science, vol. 4791. Springer, Brisbane, Australia, pp. 527–535.
- Groher, M., Jakobs, T.F., Padoy, N., Navab, N., 2007b. Planning and intraoperative visualization of liver catheterizations: new CTA protocol and 2D–3D registration method. *Acad. Radiol.* 14 (11), 1325–1340.
- Guezic, A., Kazanzides, P., Williamson, B., Taylor, R.H., 1998. Anatomy-based registration of CT-scan and intraoperative X-ray images for guiding a surgical robot. *IEEE Trans. Med. Imag.* 17 (5), 715–728.

- Guezic, A., Wu, K.N., Kalvin, A., Williamson, B., Kazanzides, P., Van Vorhis, R., 2000. Providing visual information to validate 2-D to 3-D registration. *Med. Image Anal.* 4 (4), 357–374.
- Hamadeh, A., Lavallee, S., Cinquin, P., 1998. Automated 3-dimensional computed tomographic and fluoroscopic image registration. *Comput. Aided Surg.* 3 (1), 11–19.
- Hermans, J., Claes, P., Bellemans, J., Vandermeulen, D., Suetens, P., 2007a. Robust initialization for 2D/3D registration of knee implant models to single-plane fluoroscopy. In: Pluim, J.P.W., Reinhardt, J.M. (Eds.), *Medical Imaging 2007: Image Processing*, vol. 6512. SPIE, San Diego, CA, USA, p. 651208.
- Hermans, J., Claes, P., Bellemans, J., Vandermeulen, D., Suetens, P., 2007b. A robust optimization strategy for intensity-based 2D/3D registration of knee implant models to single-plane fluoroscopy. In: Pluim, J.P.W., Reinhardt, J.M. (Eds.), *Medical Imaging 2007: Image Processing*, vol. 6512. SPIE, San Diego, CA, USA, p. 651227.
- Hill, D.L.G., Batchelor, P.G., Holden, M., Hawkes, D.J., 2001. Medical image registration. *Phys. Med. Biol.* 46 (3), R1–R45.
- Hipwell, J.H., Penney, G.P., McLaughlin, R.A., Rhode, K., Summers, P., Cox, T.C., Byrne, J.V., Noble, J.A., Hawkes, D.J., 2003. Intensity-based 2-D-3-D registration of cerebral angiograms. *IEEE Trans. Med. Imag.* 22 (11), 1417–1426.
- Ho, A.K., Fu, D., Cotrutz, C., Hancock, S.L., Chang, S.D., Gibbs, I.C., Maurer, C.R., Adler, J.R., 2007. A study of the accuracy of cyberknife spinal radiosurgery using skeletal structure tracking. *Neurosurgery* 60 (2), 147–156.
- Hoff, W.A., Komistek, R.D., Dennis, D.A., Gabriel, S.M., Walker, S.A., 1998. Three-dimensional determination of femoral-tibial contact positions under in vivo conditions using fluoroscopy. *Clin. Biomech.* 13 (7), 455–472.
- Hofstetter, R., Slomczykowski, M., Sati, M., Nolte, L.-P., 1999. Fluoroscopy as an imaging means for computer-assisted surgical navigation. *Comput. Aided Surg.* 4 (2), 65–76.
- Horn, B.K.P., 1987. Closed-form solution of absolute orientation using unit quaternions. *J. Opt. Soc. Am. A: Opt. Image Sci. Vis.* 4 (4), 629–642.
- Hummel, J., Figl, M., Bax, M., Bergmann, H., Birkfellner, W., 2008. 2D/3D registration of endoscopic ultrasound to CT volume data. *Phys. Med. Biol.* 53 (16), 4303–4316.
- Hurvitz, A., Joskowicz, L., 2008. Registration of a CT-like atlas to fluoroscopic X-ray images using intensity correspondences. *Int. J. CARS* 3 (6), 493–504.
- Imamura, H., Ida, N., Sugimoto, N., Eiho, S., Urayama, S.-i., Ueno, K., Inoue, K., 2002. Registration of preoperative CTA and intraoperative fluoroscopic images for assisting aortic stent grafting. In: Dohi, T., Kikinis, R. (Eds.), *Fifth International Conference on Medical Image Computing and Computer-Assisted Intervention (MICCAI 2002)*, Lecture Notes in Computer Science, vol. 2489. Springer, Tokyo, Japan, pp. 477–484.
- Imura, M., Yamazaki, K., Shirato, H., Onimaru, R., Fujino, M., Shimizu, S., Harada, T., Ogura, S., Dosaka-Akita, H., Miyasaka, K., Nishimura, M., 2005. Insertion and fixation of fiducial markers for setup and tracking of lung tumors in radiotherapy. *Int. J. Radiat. Oncol. Biol. Phys.* 63 (5), 1442–1447.
- Jacob, A.L., Regazzoni, P., Bilecen, D., Rasmus, M., Huegeli, R.W., Messmer, P., 2007. Medical technology integration: CT, angiography, imaging-capable OR-table, navigation and robotics in a multifunctional sterile suite. *Minim. Invasive Ther. Allied Technol.* 16 (4), 205–211.
- Jaffray, D.A., Siewerdsen, J.H., Wong, J.W., Martinez, A.A., 2002. Flat-panel cone-beam computed tomography for image-guided radiation therapy. *Int. J. Radiat. Oncol. Biol. Phys.* 53 (5), 1337–1349.
- Jaffray, D., Kupelian, P., Djemil, T., Macklis, R.M., 2007. Review of image-guided radiation therapy. *Expet. Rev. Anticancer Ther.* 7 (1), 89–103.
- Jaffray, D., Siewerdsen, J., Gospodarowicz, M., 2008. Radiation oncology. In: Peters, T.M., Cleary, K. (Eds.), *Image Guided Interventions Technology and Applications*. Springer, pp. 501–529 (Chapter 17).
- Jannin, P., Fitzpatrick, J.M., Hawkes, D.J., Pennec, X., Shahidi, R., Vannier, M.W., 2002. Validation of medical image processing in image-guided therapy. *IEEE Trans. Med. Imag.* 21 (12), 1445–1449.
- Jannin, P., Grova, C., Maurer, C., 2006a. Model for defining and reporting reference-based validation protocols in medical image processing. *Int. J. CARS* 1 (2), 63.
- Jannin, P., Krupinski, E., Warfield, S.K., 2006b. Guest editorial validation in medical image processing. *IEEE Trans. Med. Imag.* 25 (11), 1405–1409.
- Jans, H.S., Syme, A.M., Rathee, S., Fallone, B.G., 2006. 3D interfractional patient position verification using 2D–3D registration of orthogonal images. *Med. Phys.* 33 (5), 1420–1439.
- Jaramaz, B., Eckman, K., 2006. 2D/3D registration for measurement of implant alignment after total hip replacement. In: Larsen, R., Nielsen, M., Sporning, J. (Eds.), *Ninth International Conference on Medical Image Computing and Computer-Assisted Intervention (MICCAI 2006)*, Part 2, Lecture Notes in Computer Science, vol. 4191. Springer, Copenhagen, Denmark, pp. 653–661.
- Jin, J.Y., Ryu, S., Faber, K., Mikkelsen, T., Chen, Q., Li, S.D., Movsas, B., 2006. 2D/3D image fusion for accurate target localization and evaluation of a mask based stereotactic system in fractionated stereotactic radiotherapy of cranial lesions. *Med. Phys.* 33 (12), 4557–4566.
- Jolesz, F.A., 2005. Future perspectives for intraoperative MRI. *Neurosurg. Clin. N. Am.* 16 (1), 201–213.
- Jomier, J., Bullitt, E., Van Horn, M., Pathak, C., Aylward, S.R., 2006. 3D/2D model-to-image registration applied to tips surgery. In: Larsen, R., Nielsen, M., Sporning, J. (Eds.), *Ninth International Conference on Medical Image Computing and Computer-Assisted Intervention (MICCAI 2006)*, Part 2, Lecture Notes in Computer Science, vol. 4191. Springer, Copenhagen, Denmark, pp. 662–669.
- Jonic, S., Thevenaz, P., Unser, M.A., 2003. Multiresolution-based registration of a volume to a set of its projections. In: Sonka, M., Fitzpatrick, J.M. (Eds.), *Medical Imaging 2003: Image Processing*, vol. 5032. SPIE, San Diego, CA, USA, pp. 1049–1052.
- Kaptein, B.L., Valstar, E.R., Stoel, B.C., Rozing, P.M., Reiber, J.H.C., 2003. A new model-based RSA method validated using CAD models and models from reversed engineering. *J. Biomech.* 36 (6), 873–882.
- Kerrien, E., Berger, M.O., Maurincomme, E., Launay, L., Vaillant, R., Picard, L., 1999. Fully automatic 3D/2D subtracted angiography registration. In: Taylor, C., Colchester, A. (Eds.), *Second International Conference on Medical Image Computing and Computer-Assisted Intervention (MICCAI'99)*, Lecture Notes in Computer Science, vol. 1679. Springer, Cambridge, UK, pp. 664–671.
- Khamene, A., Bloch, P., Wein, W., Svatos, M., Sauer, F., 2006. Automatic registration of portal images and volumetric CT for patient positioning in radiation therapy. *Med. Image Anal.* 10 (1), 96–112.
- Kim, J., Fessler, J.A., Lam, K.L., Balter, J.M., Ten Haken, R.K., 2001. A feasibility study of mutual information based setup error estimation for radiotherapy. *Med. Phys.* 28 (12), 2507–2517.
- Kim, J., Yin, F.F., Zhao, Y., Kim, J.H., 2005. Effects of X-ray and CT image enhancements on the robustness and accuracy of a rigid 3D/2D image registration. *Med. Phys.* 32 (4), 866–873.
- Kim, J., Li, S.D., Pradhan, D., Hammoud, R., Chen, Q., Yin, F.F., Zhao, Y., Kim, J.H., Movsas, B., 2007. Comparison of similarity measures for rigid-body CT/dual X-ray image registrations. *Technol. Cancer Res. Treat.* 6 (4), 337–345.
- Kirby, M.C., Glendinning, A.G., 2006. Developments in electronic portal imaging systems. *Brit. J. Radiol.* 79, S50–S65.
- Kita, Y., Wilson, D.L., Noble, J.A., 1998. Real-time registration of 3D cerebral vessels to X-ray angiograms. In: Wells, W., Colchester, A., Delp, S. (Eds.), *First International Conference on Medical Image Computing and Computer-Assisted Intervention (MICCAI'98)*, Lecture Notes in Computer Science, vol. 1496. Springer, Cambridge, MA, USA, pp. 1125–1133.
- Knaan, D., Joskowicz, L., 2003. Effective intensity-based 2D/3D rigid registration between fluoroscopic X-ray and CT. In: Ellis, R., Peters, T.M. (Eds.), *Sixth International Conference on Medical Image Computing and Computer-Assisted Intervention (MICCAI 2003)*, Part 1, Lecture Notes in Computer Science, vol. 2878. Springer, Montreal, Canada, pp. 351–358.
- Kubias, A., Deinzer, F., Feldmann, T., Paulus, D., 2007. Extended global optimization strategy for rigid 2D/3D image registration. In: Kropatsch, W., Kampel, M., Hanbury, A. (Eds.), *12th International Conference on Computer Analysis of Images and Patterns (CAIP 2007)*, Lecture Notes in Computer Science, vol. 4673. Springer, Vienna, Austria, pp. 759–767.
- Lamecker, H., Wenckebach, T.H., Hege, H., 2006. Atlas-based 3D-shape reconstruction from X-ray images. In: *Proceedings of the 18th International Conference on Pattern Recognition (ICPR 2006)*. IEEE Computer Society, Washington, DC, USA, pp. 371–374.
- LaRose, D., 2001. Iterative X-ray/CT registration using accelerated volume rendering. Ph.D. Thesis, Robotics Institute, Carnegie Mellon University, Pittsburgh, PA.
- LaRose, D., Bayouth, J., Kanade, T., 2000a. Transgraph: interactive intensity-based 2D/3D registration of X-ray and CT data. In: Hanson, K.M. (Ed.), *Medical Imaging 2000: Image Processing*, vol. 3979. SPIE, San Diego, CA, USA, pp. 385–396.
- LaRose, D., Cassenti, L., Jaramaz, B., Moody Jr., J., Kanade, T., DiGioia, A., 2000b. Post-operative measurement of acetabular cup position using X-ray/CT registration. In: Delp, S.L., DiGioia, A.M., Jaramaz, B. (Eds.), *Third International Conference on Medical Image Computing and Computer-Assisted Intervention (MICCAI 2000)*, Lecture Notes in Computer Science, vol. 1935. Springer, Pittsburgh, PA, USA, pp. 1104–1113.
- Lavallee, S., Szelski, R., 1995. Recovering the position and orientation of free-form objects from image contours using 3D distance maps. *IEEE Trans. Pattern Anal. Mach. Intell.* 17 (4), 378–390.
- Lemieux, L., Jagoe, R., Fish, D.R., Kitchen, N.D., Thomas, D.G.T., 1994. A patient-to-computed-tomography image registration method based on digitally reconstructed radiographs. *Med. Phys.* 21 (11), 1749–1760.
- Levoy, M., Hanrahan, P., 1994. Light field rendering. In: *Proceedings of the 23rd Annual Conference on Computer Graphics and Interactive Techniques (SIGGRAPH 1996)*. ACM Press, New York, NY, USA, pp. 31–42.
- Liao, R., Guetter, C., Xu, C.Y., Sun, Y.Y., Khamene, A., Sauer, F., 2006. Learning-based 2D/3D rigid registration using Jensen-Shannon divergence for image-guided surgery. In: Yang, G., Jiang, T., Shen, D., Gu, L., Yang, G. (Eds.), *Third International Workshop on Medical Imaging and Augmented Reality*, Lecture Notes in Computer Science, vol. 4091. Springer, Shanghai, China, pp. 228–235.
- Li, X.L., Yang, J., Zhu, Y.M., 2006. Digitally reconstructed radiograph generation by an adaptive Monte Carlo method. *Phys. Med. Biol.* 51 (11), 2745–2752.
- Litzenberg, D., Dawson, L.A., Sandler, H., Sanda, M.G., McShan, D., Ten Haken, R.K., Lam, K.L., Brock, K.K., Balter, J.M., 2002. Daily prostate targeting using implanted radiopaque markers. *Int. J. Radiat. Oncol. Biol. Phys.* 52 (3), 699–703.
- Liu, A., Bullitt, E., Pizer, S.M., 1998. 3D/2D registration via skeletal near projective invariance in tubular objects. In: Wells, W., Colchester, A., Delp, S. (Eds.), *First International Conference on Medical Image Computing and Computer-Assisted Intervention (MICCAI'98)*, Lecture Notes in Computer Science, vol. 1496. Springer, Cambridge, MA, USA, pp. 952–963.
- Livyatan, H., Yaniv, Z., Joskowicz, L., 2002. Robust automatic C-arm calibration for fluoroscopy-based navigation: a practical approach. In: Dohi, T., Kikinis, R. (Eds.), *Fifth International Conference on Medical Image Computing and Computer-Assisted Intervention (MICCAI 2002)*, Lecture Notes in Computer Science, vol. 2489. Springer, Tokyo, Japan, pp. 60–68.
- Livyatan, H., Yaniv, Z., Joskowicz, L., 2003. Gradient-based 2-D/3-D rigid registration of fluoroscopic X-ray to CT. *IEEE Trans. Med. Imag.* 22 (11), 1395–1406.

- Maes, F., Collignon, A., Vandermeulen, D., Marchal, G., Suetens, P., 1997. Multimodality image registration by maximization of mutual information. *IEEE Trans. Med. Imag.* 16 (2), 187–198.
- Mahfouz, M.R., Hoff, W.A., Komistek, R.D., Dennis, D.A., 2003. A robust method for registration of three-dimensional knee implant models to two-dimensional fluoroscopy images. *IEEE Trans. Med. Imag.* 22 (12), 1561–1574.
- Mahfouz, M.R., Hoff, W.A., Komistek, R.D., Dennis, D.A., 2005. Effect of segmentation errors on 3D-to-2D registration of implant models in X-ray images. *J. Biomech.* 38 (2), 229–239.
- Maintz, J.B., Viergever, M.A., 1998. A survey of medical image registration. *Med. Image Anal.* 2 (1), 1–36.
- Markelj, P., Tomažević, D., Pernuš, F., Likar, B., 2007. Optimizing bone extraction in MR images for 3D/2D gradient based registration of MR and X-ray images. In: Reinhardt, J., Pluim, J. (Eds.), *Medical Imaging 2007: Image Processing*, vol. 6512. SPIE, San Diego, CA, USA, p. 651224.
- Markelj, P., Tomažević, D., Pernuš, F., Likar, B., 2008. Robust gradient-based 3-D/2-D registration of CT and MR to X-ray images. *IEEE Trans. Med. Imag.* 27 (12), 1704–1714.
- Maurer, C.R., Fitzpatrick, J.M., 1993. A review of medical image registration. In: Maciunas, J. (Ed.), *Interactive Image-Guided Neurosurgery*. American Association of Neurological Surgeons, Park Ridge, IL, USA, pp. 17–44.
- Maurer, C.R., Fitzpatrick, J.M., Wang, M.Y., Galloway, R.L., Maciunas, R.J., Allen, G.S., 1997. Registration of head volume images using implantable fiducial markers. *IEEE Trans. Med. Imag.* 16 (4), 447–462.
- Mauro, M.A., Murphy, K., Thomson, K., Venbrux, A., Zollkofer, C.L. (Eds.), 2008. *Image-Guided Intervention, 2-Volume Set, Expert Radiology*, Saunders.
- Mayberg, M., LaPresto, E., Cunningham, E., 2005. Image-guided endoscopy: description of technique and potential applications. *Neurosurg. Focus* 19 (1), E10.
- McLaughlin, R.A., Hipwell, J., Hawkes, D.J., Noble, J.A., Byrne, J.V., Cox, T.C., 2005. A comparison of a similarity-based and a feature-based 2-D-3-D registration method for neurointerventional use. *IEEE Trans. Med. Imag.* 24 (8), 1058–1066.
- Micu, R., Jakobs, T.F., Urschler, M., Navab, N., 2006. A new registration/visualization paradigm for CT-fluoroscopy guided RF liver ablation. In: Larsen, R., Nielsen, M., Sporning, J. (Eds.), *Ninth International Conference on Medical Image Computing and Computer-Assisted Intervention (MICCAI 2006)*, Part 1, Lecture Notes In Computer Science, vol. 4190. Springer, Copenhagen, Denmark, pp. 882–890.
- Miga, M.I., Sinha, T.K., Cash, D.M., Galloway, R.L., Weil, R.J., 2003. Cortical surface registration for image-guided neurosurgery using laser-range scanning. *IEEE Trans. Med. Imag.* 22 (8), 973–985.
- Miquel, M.E., Rhode, K.S., Acher, P.L., MacDougall, N.D., Blackall, J., Gaston, R.P., Hegde, S., Morris, S.L., Beaney, R., Deehan, C., Popert, R., Keevil, S.F., 2006. Using combined X-ray and MR imaging for prostate I-125 post-implant dosimetry: phantom validation and preliminary patient work. *Phys. Med. Biol.* 51 (5), 1129–1137.
- Mori, K., Deguchi, D., Sugiyama, J., Suenaga, Y., Toriwaki, J., Maurer, C.R., Takabatake, H., Natori, H., 2002. Tracking of a bronchoscope using epipolar geometry analysis and intensity-based image registration of real and virtual endoscopic images. *Med. Image Anal.* 6 (3), 321–336.
- Mori, K., Deguchi, D., Akiyama, K., Kitasaka, T., Maurer, C.R., Suenaga, Y., Takabatake, H., Mori, M., Natori, H., 2005. Hybrid bronchoscope tracking using a magnetic tracking sensor and image registration. In: Duncan, J.S., Gerig, G. (Eds.), *Eighth International Conference on Medical Image Computing and Computer-Assisted Intervention (MICCAI 2005)*, Part 2, Lecture Notes In Computer Science, vol. 3750. Springer, Palm Springs, PA, USA, pp. 543–550.
- Mu, Z.P., Fu, D.S., Kuduvali, G., 2008. A probabilistic framework based on hidden markov model for fiducial identification in image-guided radiation treatments. *IEEE Trans. Med. Imag.* 27 (9), 1288–1300.
- Munbodh, R., Jaffray, D.A., Moseley, D.J., Chen, Z., Knisely, J.P.S., Cathier, P., Duncan, J.S., 2006. Automated 2D–3D registration of a radiograph and a cone beam CT using line-segment enhancement. *Med. Phys.* 33 (5), 1398–1411.
- Munbodh, R., Chen, Z., Jaffray, D.A., Moseley, D.J., Knisely, J.P.S., Duncan, J.S., 2007. A frequency-based approach to locate common structure for 2D–3D intensity-based registration of setup images in prostate radiotherapy. *Med. Phys.* 34 (7), 3005–3017.
- Munbodh, R., Chen, Z., Jaffray, D.A., Moseley, D.J., Knisely, J.P.S., Duncan, J.S., 2008. Automated 2D–3D registration of portal images and CT data using line-segment enhancement. *Med. Phys.* 35 (10), 4352–4361.
- Munbodh, R., Tagare, H.D., Chen, Z., Jaffray, D.A., Moseley, D.J., Knisely, J.P.S., Duncan, J.S., 2009. 2D–3D registration for prostate radiation therapy based on a statistical model of transmission images. *Med. Phys.* 36 (10), 4555–4568.
- Murphy, M.J., 1997. An automatic six-degree-of-freedom image registration algorithm for image-guided frameless stereotaxic radiosurgery. *Med. Phys.* 24 (6), 857–866.
- Murphy, M.J., 1999. The importance of computed tomography slice thickness in radiographic patient positioning for radiosurgery. *Med. Phys.* 26 (2), 171–175.
- Murphy, M.J., 2002. Fiducial-based targeting accuracy for external-beam radiotherapy. *Med. Phys.* 29 (3), 334–344.
- Murphy Jr., M.J., Adler, J.R., Bodduluri, M., Dooley, J., Forster, K., Hai, J., Le, Q., Luxton, G., Martin, D., Poen, J., 2000. Image-guided radiosurgery for the spine and pancreas. *Comput. Aided Surg.* 5 (4), 278–288.
- Nakajima, Y., Tamura, Y., Sato, Y., Tashiro, T., Sugano, N., Yonenobu, K., Yoshikawa, H., Ochi, T., Tamura, S., 2002. Preoperative analysis of optimal imaging orientation in fluoroscopy for voxel-based 2-D/3-D registration. In: Dohi, T., Kikinis, R. (Eds.), *Fifth International Conference on Medical Image Computing and Computer-Assisted Intervention (MICCAI 2002)*, Lecture Notes in Computer Science, vol. 2489. Springer, Tokyo, Japan, pp. 485–492.
- Nakajima, Y., Tashiro, T., Sugano, N., Yonenobu, K., Koyama, T., Maeda, Y., Tamura, Y., Saito, M., Tamura, S., Mitsuishi, M., Sugita, N., Sakuma, I., Ochi, T., Matsumoto, Y., 2007. Fluoroscopic bone fragment tracking for surgical navigation in femur fracture reduction by incorporating optical tracking of hip joint rotation center. *IEEE Trans. Biomed. Eng.* 54 (9), 1703–1706.
- Nicolau, S., Pennec, X., Soler, L., Buy, X., Gangi, A., Ayache, N., Marescaux, J., 2009. An augmented reality system for liver thermal ablation: design and evaluation on clinical cases. *Med. Image Anal.* 13 (3), 494–506.
- Pawiro, S., Markelj, P., Gendrin, C., Figl, M., Stock, M., Bloch, C., Weber, C., Unger, E., Nöbauer, I., Kainberger, F., Bergmeister, H., Georg, D., Bergmann, H., Birkfellner, W., 2010. A new gold-standard dataset for 2D/3D image registration evaluation. In: Wong, K.H., Miga, M.I. (Eds.), *Medical Imaging 2010: Image Processing*, vol. 7625. SPIE, San Diego, CA, USA, p. 76251V.
- Penney, G.P., Weese, J., Little, J.A., Desmedt, P., Hill, D.L.G., Hawkes, D.J., 1998. A comparison of similarity measures for use in 2-D–3-D medical image registration. *IEEE Trans. Med. Imag.* 17 (4), 586–595.
- Penney, G.P., Batchelor, P.G., Hill, D.L.G., Hawkes, D.J., Weese, J., 2001. Validation of a two- to three-dimensional registration algorithm for aligning preoperative CT images and intraoperative fluoroscopy images. *Med. Phys.* 28 (6), 1024–1032.
- Penney, G.P., Barratt, D.C., Chan, C.S.K., Slomczykowski, M., Carter, T.J., Edwards, P.J., Hawkes, D.J., 2006. Cadaver validation of intensity-based ultrasound to CT registration. *Med. Image Anal.* 10 (3), 385–395.
- Penney, G.P., Edwards, P.J., Hipwell, J.H., Slomczykowski, M., Revie, I., Hawkes, D.J., 2007. Postoperative calculation of acetabular cup position using 2-D–3-D registration. *IEEE Trans. Biomed. Eng.* 54 (7), 1342–1348.
- Peters, T.M., 2006. Image-guidance for surgical procedures. *Phys. Med. Biol.* 51 (14), R505–R540.
- Peters, T.M., Cleary, K. (Eds.), 2008. *Image Guided Interventions, Technology and Applications*. Springer.
- Pluim, J.P.W., Maintz, J.B.A., Viergever, M.A., 2003. Mutual-information-based registration of medical images: a survey. *IEEE Trans. Med. Imag.* 22 (8), 986–1004.
- Pouliot, J., Bani-Hashemi, A., Chen, J., Svatos, M., Ghelmsarai, F., Mitschke, M., Aubin, M., Xia, P., Morin, O., Bucci, K., Roach, M., Hernandez, P., Zheng, Z.R., Hristov, D., Verhey, L., 2005. Low-dose megavoltage cone-beam CT for radiation therapy. *Int. J. Radiat. Oncol. Biol. Phys.* 61 (2), 552–560.
- Prümmer, M., Hornegger, J., Pfister, M., Dörfler, A., 2006. Multi-modal 2D–3D non-rigid registration. In: Reinhardt, J., Pluim, J. (Eds.), *Medical Imaging 2006: Image Processing*, vol. 6144. SPIE, San Diego CA, USA, p. 61440X.
- Qi, W., Gu, L., Xu, J., 2008. Non-rigid 2D-3D registration based on support vector regression estimated similarity metric. In: Dohi, T., Sakuma, I., Liao, H. (Eds.), *Fourth International Workshop on Medical Imaging and Augmented Reality*, Lecture Notes in Computer Science, vol. 5128. Springer, Tokyo, Japan, pp. 339–348.
- Remeijer, P., Geerlof, E., Ploeger, L., Gilhuijs, K., van Herk, M., Lebesque, J.V., 2000. 3-D portal image analysis in clinical practice: an evaluation of 2-D and 3-D analysis techniques as applied to 30 prostate cancer patients. *Int. J. Radiat. Oncol. Biol. Phys.* 46 (5), 1281–1290.
- Rezk-Salama, C., Engel, K., Bauer, M., Greiner, G., Ertl, T., 2000. Interactive volume on standard PC graphics hardware using multi-textures and multi-stage rasterization. In: *Proceedings of the ACM SIGGRAPH/EUROGRAPHICS Workshop on Graphics Hardware*. ACM Press, Interlaken, Switzerland, pp. 109–118.
- Rhode, K.S., Hill, D.L.G., Edwards, P.J., Hipwell, J., Rueckert, D., Sanchez-Ortiz, G., Hegde, S., Rahunathan, V., Razavi, R., 2003. Registration and tracking to integrate X-ray and MR images in an XMR facility. *IEEE Trans. Med. Imag.* 22 (11), 1369–1378.
- Rhode, K.S., Sermesant, M., Brogan, D., Hegde, S., Hipwell, J., Lambiase, P., Rosenthal, E., Bucknall, C., Qureshi, S.A., Gill, J.S., Razavi, R., Hill, D.L.G., 2005. A system for real-time XMR guided cardiovascular intervention. *IEEE Trans. Med. Imag.* 24 (11), 1428–1440.
- Rohlfing, T., Maurer, C., 2002. A novel image similarity measure for registration of 3-D MR images and X-ray projection images. In: Dohi, T., Kikinis, R. (Eds.), *Fifth International Conference on Medical Image Computing and Computer-Assisted Intervention (MICCAI 2002)*, Lecture Notes in Computer Science, vol. 2489. Springer, Tokyo, Japan, pp. 469–476.
- Rohlfing, T., Russakoff, D.B., Denzler, J., Maurer, C.R., 2004. Progressive attenuation fields: Fast 2D–3D image registration without precomputation. In: Barillot, C., Haynor, D.R., Hellier, P. (Eds.), *Seventh International Conference on Medical Image Computing and Computer-Assisted Intervention (MICCAI 2004)*, Part 1, Lecture Notes In Computer Science, vol. 3216. Springer, Saint-Malo, France, pp. 631–638.
- Rohlfing, T., Denzler, J., Grassl, C., Russakoff, D.B., Maurer, C.R., 2005a. Markerless real-time 3-D target region tracking by motion backprojection from projection images. *IEEE Trans. Med. Imag.* 24 (11), 1455–1468.
- Rohlfing, T., Russakoff, D.B., Denzler, J., Mori, K., Maurer, C.R., 2005b. Progressive attenuation fields: fast 2D–3D image registration without precomputation. *Med. Phys.* 32 (9), 2870–2880.
- Romanelli, P., Schaal, D.W., Adler, J.R., 2006a. Image-guided radiosurgical ablation of intra- and extra-cranial lesions. *Technol. Cancer Res. Treat.* 5 (4), 421–428.
- Romanelli, P., Schweikard, A., Schlaefer, A., Adler, J., 2006b. Computer aided robotic radiosurgery. *Comput. Aided Surg.* 11 (4), 161–174.
- Roth, M., Brack, C., Burgkart, R., Czopf, A., 1999. Multi-view contourless registration of bone structures using a single calibrated X-ray fluoroscope. In: Lemke, H.U.,

- Vannier, M.W., Inamura, K., Farman, A.G. (Eds.), CARS 1999: Computer Assisted Radiology and Surgery. Proceedings of the 13th International Congress and Exhibition, International Congress Series, vol. 1191. Elsevier, Paris, France, p. 756761.
- Russakoff, D.B., Rohlfing, T., Ho, A., Kim, D.H., Shahidi, R., Adler, J.R., Maurer, C.R., 2003. Evaluation of intensity-based 2D–3D spine image registration using clinical gold-standard data. In: Gee, J.C., Maintz, J.B.A., Vannier, M.W. (Eds.), Second International Workshop on Biomedical Image Registration (WBIR2003), Lecture Notes In Computer Science, vol. 2717. Springer, Philadelphia, PA, USA, pp. 151–160.
- Russakoff, D.B., Rohlfing, T., Adler, J.R., Maurer, C.R., 2005a. Intensity-based 2D–3D spine image registration incorporating a single fiducial marker. *Acad. Radiol.* 12 (1), 37–50.
- Russakoff, D.B., Rohlfing, T., Mori, K., Rueckert, D., Ho, A., Adler, J.R., Maurer, C.R., 2005b. Fast generation of digitally reconstructed radiographs using attenuation fields with application to 2D–3D image registration. *IEEE Trans. Med. Imag.* 24 (11), 1441–1454.
- Sadowsky, O., Ramamurthi, K., Ellingsen, L., Chintalapani, G., Prince, J., Taylor, R., 2006. Atlas-assisted tomography: registration of a deformable atlas to compensate for limited-angle cone-beam trajectory. In: Third IEEE International Symposium on Biomedical Imaging: Nano to Macro, ISBI2006. IEEE Computer Society Press, pp. 1244–1247.
- Sadowsky, O., Chintalapani, G., Taylor, R., 2007. Deformable 2D–3D registration of the pelvis with a limited field of view, using shape statistics. In: Ayache, N., Ourselin, S., Maeder, A. (Eds.), 10th International Conference on Medical Image Computing and Computer-Assisted Intervention (MICCAI 2007), Lecture Notes In Computer Science, vol. 4792. Springer, Brisbane, Australia, pp. 519–526.
- Sarrut, D., Clippe, S., 2001. Geometrical transformation approximation for 2D/3D intensity-based registration of portal images and CT scan. In: Niessen, W.J., Viereger, M.A. (Eds.), Fourth International Conference on Medical Image Computing and Computer-Assisted Intervention (MICCAI 2001), Lecture Notes in Computer Science, vol. 2208. Springer, Utrecht, The Netherlands, pp. 532–540.
- Sauer, F., 2005. Image registration: enabling technology for image guided surgery and therapy. In: 27th Annual International Conference on Engineering in Medicine and Biology Society, 2005 (IEEE-EMBS 2005), pp. 7242–7245.
- Schweikard, A., Shiomi, H., Adler, J., 2004. Respiration tracking in radiosurgery. *Med. Phys.* 31 (10), 2738–2741.
- Schweikard, A., Shiomi, H., Adler, J., 2005. Respiration tracking in radiosurgery without fiducials. *Int. J. Med. Robot. Comput. Assist. Surg.* 1 (2), 19–27.
- Shirato, H., Shimizu, S., Kitamura, K., Nishioka, T., Kagei, K., Hashimoto, S., Aoyama, H., Kunieda, T., Shinohara, N., Dosaka-Akita, H., Miyasaka, K., 2000. Four-dimensional treatment planning and fluoroscopic real-time tumor tracking radiotherapy for moving tumor. *Int. J. Radiat. Oncol. Biol. Phys.* 48 (2), 435–442.
- Sirois, L.M., Hristov, D.H., Fallone, B.G., 1999. Three-dimensional anatomy setup verification by correlation of orthogonal portal images and digitally reconstructed radiographs. *Med. Phys.* 26 (11), 2422–2428.
- Škerl, D., Tomažević, D., Likar, B., Pernuš, F., 2006. Evaluation of similarity measures for reconstruction-based registration in image-guided radiotherapy and surgery. *Int. J. Radiat. Oncol. Biol. Phys.* 65 (3), 943–953.
- Skrinjar, O., 2006. Point-based registration with known correspondence: closed form optimal solutions and properties. In: Plum, J., Likar, B., Gerritsen, F. (Eds.), Third International Workshop on Biomedical Image Registration (WBIR2006), Lecture Notes In Computer Science, vol. 4057. Springer, Utrecht, The Netherlands, pp. 315–321.
- Soete, G., Van de Steene, J., Verellen, D., Vinh-Hung, V., Van den Berge, D., Michielsens, D., Keuppens, F., De Roover, P., Storme, G., 2002. Initial clinical experience with infrared-reflecting skin markers in the positioning of patients treated by conformal radiotherapy for prostate cancer. *Int. J. Radiat. Oncol. Biol. Phys.* 52 (3), 694–698.
- Spoerk, J., Bergmann, H., Wanschitz, F., Dong, S., Birkfellner, W., 2007. Fast DRR splat rendering using common consumer graphics hardware. *Med. Phys.* 34 (11), 4302–4308.
- Sundar, H., Khamene, A., Xu, C., Sauer, F., Davatzikos, C., 2006. A novel 2D–3D registration algorithm for aligning fluoro images with 3D pre-op CT/MR images. *Medical Imaging 2006: Visualization, Image-Guided Procedures, and Display*, vol. 6141. SPIE, San Diego, CA, USA, p. 61412K.
- Sun, H., Lunn, K.E., Farid, H., Wu, Z.J., Roberts, D.W., Hartov, A., Paulsen, K.D., 2005. Stereopsis-guided brain shift compensation. *IEEE Trans. Med. Imag.* 24 (8), 1039–1052.
- Tang, T.S.Y., Ellis, R.E., 2005. 2D/3D deformable registration using a hybrid atlas. In: Duncan, J.S., Gerig, G. (Eds.), Eighth International Conference on Medical Image Computing and Computer-Assisted Intervention (MICCAI 2005), Part 2, Lecture Notes In Computer Science, vol. 3750. Springer, Palm Springs, CA, USA, pp. 223–230.
- Tang, T., Ellis, R., Fichtinger, G., 2000. Fiducial registration from a single X-ray image: A new technique for fluoroscopic guidance and radiotherapy. In: Delp, S.L., DiGioia, A.M., Jaramaz, B. (Eds.), Third International Conference on Medical Image Computing and Computer-Assisted Intervention (MICCAI 2000), Lecture Notes In Computer Science, vol. 1935. Springer, Pittsburgh, PA, USA, pp. 502–511.
- Tang, T., MacIntyre, N., Gill, H., Fellows, R., Hill, N., Wilson, D., Ellis, R., 2004a. Hardware-assisted 2D/3D intensity-based registration for assessing patellar tracking. In: Barillot, C., Haynor, D.R., Hellier, P. (Eds.), Seventh International Conference on Medical Image Computing and Computer-Assisted Intervention (MICCAI 2004), Part 2, Lecture Notes In Computer Science, vol. 3217. Springer, Saint-Malo, France, pp. 1095–1096.
- Tang, T.S.Y., MacIntyre, N.J., Gill, H.S., Fellows, R.A., Hill, N.A., Wilson, D.R., Ellis, R.E., 2004b. Accurate assessment of patellar tracking using fiducial and intensity-based fluoroscopic techniques. *Med. Image Anal.* 8 (3), 343–351.
- Tomažević, D., Likar, B., Slivnik, T., Pernuš, F., 2003. 3-D/2-D registration of CT and MR to X-ray images. *IEEE Trans. Med. Imag.* 22 (11), 1407–1416.
- Tomažević, D., Likar, B., Pernuš, F., 2004. "Gold standard" data for evaluation and comparison of 3D/2D registration methods. *Comput. Aided Surg.* 9 (4), 137–144.
- Tomažević, D., Likar, B., Pernuš, F., 2006. 3-D/2-D registration by integrating 2-D information in 3-D. *IEEE Trans. Med. Imag.* 25 (1), 17–27.
- Tomažević, D., Likar, B., Pernuš, F., 2007. 3D/2D image registration: The impact of X-ray views and their number. In: Ayache, N., Ourselin, S., Maeder, A. (Eds.), 10th International Conference on Medical Image Computing and Computer-Assisted Intervention (MICCAI 2007), Lecture Notes In Computer Science, vol. 4791. Springer, Brisbane, Australia, pp. 450–457.
- Turgeon, G.A., Lehmann, G., Guiraudon, G., Drangova, M., Holdsworth, D., Peters, T., 2005. 2D–3D registration of coronary angiograms for cardiac procedure planning and guidance. *Med. Phys.* 32 (12), 3737–3749.
- Umeyama, S., 1991. Least-squares estimation of transformation parameters between 2 point patterns. *IEEE Trans. Pattern Anal. Mach. Intell.* 13 (4), 376–380.
- van de Kraats, E.B., Penney, G.P., Tomažević, D., van Walsum, T., Niessen, W.J., 2005a. Standardized evaluation methodology for 2-D–3-D registration. *IEEE Trans. Med. Imag.* 24 (9), 1177–1189.
- van de Kraats, E.B., Penney, G.P., van Walsum, T., Niessen, W.J., 2005b. Multispectral MR to X-ray registration of vertebral bodies by generating CT-like data. In: Duncan, J.S., Gerig, G. (Eds.), Eighth International Conference on Medical Image Computing and Computer-Assisted Intervention (MICCAI 2005), Part 2, Lecture Notes In Computer Science, vol. 3750. Springer, Palm Springs, CA, USA, pp. 911–918.
- van de Kraats, E.B., van Walsum, T., Kendrick, L., Noordhoek, N.J., Niessen, W.J., 2006. Accuracy evaluation of direct navigation with an isocentric 3D rotational X-ray system. *Med. Image Anal.* 10 (2), 113.
- Vermandel, M., Betrouni, N., Gaurvit, J.Y., Pasquier, D., Vasseur, C., Rousseau, J., 2006. Intrinsic 2D/3D registration based on a hybrid approach: use in the radiosurgical imaging process. *Cell. Mol. Biol.* 52 (6), 44–53.
- Weese, J., Buzug, T.M., Lorenz, C., Fassnacht, C., 1997a. An approach to 2D/3D registration of a vertebra in 2D X-ray fluoroscopies with 3D CT images. In: Trocraz, J., Grimson, E., Mösges, R. (Eds.), CVRMed-MRCSA'97: First Joint Conference, Computer Vision, Virtual Reality and Robotics in Medicine and Medical Robotics and Computer-Assisted Surgery, Lecture Notes In Computer Science, vol. 1205. Springer, Grenoble, France, pp. 119–128.
- Weese, J., Penney, G.P., Desmedt, P., Buzug, T.M., Hill, D.L.G., Hawkes, D.J., 1997b. Voxel-based 2-D/3-D registration of fluoroscopy images and CT scans for image-guided surgery. *IEEE Trans. Inf. Technol. Biomed.* 1 (4), 284.
- Weese, J., Göcke, R., Penney, G.P., Desmedt, P., Buzug, T.M., Schumann, H., 1999. Fast voxel-based 2D/3D registration algorithm using a volume rendering method based on the shear-warp factorization. In: Hanson, K.M. (Ed.), *Medical Imaging 1999: Image Processing*, vol. 3661. SPIE, San Diego, CA, USA, pp. 802–810.
- Wein, W., Roeper, B., Navab, N., 2005. 2D/3D registration based on volume gradients. In: Fitzpatrick, J.M., Reinhardt, J.M. (Eds.), *Medical Imaging 2005: Image Processing*, vol. 5747. SPIE, San Diego, CA, USA, pp. 144–150.
- Wein, W.G., Brunke, S., Khamene, A., Callstrom, M.R., Navab, N., 2008. Automatic CT-ultrasound registration for diagnostic imaging and image-guided intervention. *Med. Image Anal.* 12 (5), 577–585.
- West, J., Fitzpatrick, J.M., Wang, M.Y., Dawant, B.M., Maurer, C.R., Kessler, R.M., Maciunas, R.J., Barillot, C., Lemoine, D., Collignon, A., Maes, F., Suetens, P., Vandenmeulen, D., vandenElsen, P.A., Napel, S., Sumanaweera, T.S., Harkness, B., Hemler, P.F., Hill, D.L.G., Hawkes, D.J., Studholme, C., Maintz, J.B.A., Viereger, M.A., Malandain, G., Pennec, X., Noz, M.E., Maguire, G.Q., Pollack, M., Pelizzari, C.A., Robb, R.A., Hanson, D., Woods, R.P., 1997. Comparison and evaluation of retrospective intermodality brain image registration techniques. *J. Comput. Assist. Tomo.* 21 (4), 554–566.
- Wunsch, P., Hinzinger, G., 1996. Registration of CAD-models to images by iterative inverse perspective matching. *Proceedings of the 1996 International Conference on Pattern Recognition (ICPR'96) Volume I*, vol. 7270. IEEE Computer Society, Washington, DC, USA, p. 78.
- Yamazaki, T., Watanabe, T., Nakajima, Y., Sugamoto, K., Tomita, T., Yoshikawa, H., Tamura, S., 2004. Improvement of depth position in 2-D/3-D registration of knee implants using single-plane fluoroscopy. *IEEE Trans. Med. Imag.* 23 (5), 602–612.
- Yaniv, Z., Cleary, K., 2006. Image guided procedures: a review. Technical Report CAIMR TR-2006-3, Georgetown University, Imaging Science and Information Systems Center, Washington, DC, USA.
- Yao, J., Taylor, R., 2003. Assessing accuracy factors in deformable 2D/3D medical image registration using a statistical pelvis model. In: Ninth IEEE International Conference on Computer Vision (ICCV 03), vol. 2, pp. 1329–1334.
- Yin, F.F., Gao, Q.H., Xie, H.C., Nelson, D.F., Yu, Y., Kwok, W.E., Totterman, S., Schell, M.C., Rubin, P., 1998. MR image-guided portal verification for brain treatment field. *Int. J. Radiat. Oncol. Biol. Phys.* 40 (3), 703–711.
- You, B.M., Siy, P., Anderst, W., Tashman, S., 2001. In vivo measurement of 3-D skeletal kinematics from sequences of biplane radiographs: Application to knee kinematics. *IEEE Trans. Med. Imag.* 20 (6), 514–525.

- Zhang, X., Zheng, G.Y., Langlotz, F., Nolte, L.P., 2006. Assessment of spline-based 2D–3D registration for image-guided spine surgery. *Minim. Invasive Ther. Allied Technol.* 15 (3), 193–199.
- Zheng, G., 2008. Effective incorporation of spatial information in a mutual information based 3D–2D registration of a CT volume to X-ray images. In: Metaxas, D., Axel, L., Fichtinger, G., Székely, G. (Eds.), 11th International Conference on Medical Image Computing and Computer-Assisted Intervention (MICCAI 2008), Lecture Notes In Computer Science, vol. 5242. Springer, New York, USA, pp. 922–929.
- Zheng, G.Y., Ballester, M.A.G., Styner, M., Nolte, L.P., 2006a. Reconstruction of patient-specific 3D bone surface from 2D calibrated fluoroscopic images and point distribution model. In: Larsen, R., Nielsen, M., Sporring, J. (Eds.), Ninth International Conference on Medical Image Computing and Computer-Assisted Intervention (MICCAI 2006), Part 1, Lecture Notes In Computer Science, vol. 4190. Springer, Copenhagen, Denmark, pp. 25–32.
- Zheng, G.Y., Zhang, X., Jonic, S., Thevenaz, P., Unser, M., Nolte, L.P., 2006b. Point similarity measures based on MRF modeling of difference images for spline-based 2D–3D rigid registration of X-ray fluoroscopy to CT images. In: Pluim, J., Likar, B., Gerritsen, F. (Eds.), Third International Workshop on Biomedical Image Registration (WBIR2006), Lecture Notes In Computer Science, vol. 4057. Springer, Utrecht, The Netherlands, pp. 186–194.
- Zheng, G.Y., Dong, X., Gonzalez Ballester, M.A.G., 2007. Unsupervised reconstruction of a patient-specific surface model of a proximal femur from calibrated fluoroscopic images. In: Ayache, N., Ourselin, S., Maeder, A. (Eds.), 10th International Conference on Medical Image Computing and Computer-Assisted Intervention (MICCAI 2007), Lecture Notes In Computer Science, vol. 4791. Springer, Brisbane, Australia, pp. 834–841.
- Zikic, D., Groher, M., Khamene, A., Navab, N., 2008. Deformable registration of 3D vessel structures to a single projection image. In: Reinhardt, J.M., Pluim, J.P.W. (Eds.), *Medical Imaging 2008: Image Processing*, vol. 6914. SPIE, San Diego, CA, USA, p. 691412.
- Zinreich, S.J., Tebo, S.A., Long, D.M., Brem, H., Mattox, D.E., Loury, M., van der Kolk, C.A., Koch, W.M., Kennedy, D.W., Bryan, R.N., 1993. Frameless stereotaxic integration of CT imaging data: accuracy and initial applications. *Radiology* 188, 735–742.
- Zöllei, L., Grimson, E., Norbash, A., Wells, W., 2001. 2D–3D rigid registration of X-ray fluoroscopy and CT images using mutual information and sparsely sampled histogram estimators. In: 2001 IEEE Computer Society Conference on Computer Vision and Pattern Recognition (CVPR'01), vol. 2, p. 696.
- Zuffi, S., Leardini, A., Catani, F., Fantozzi, S., Cappello, A., 1999. A model-based method for the reconstruction of total knee replacement kinematics. *IEEE Trans. Med. Imag.* 18 (10), 981–991.